THERMODYNAMIC AND MASS TRANSFER STUDIES

I. An Apparatus to Determine the Volumetric Behavior of Nitrogen Oxides

II. Isobaric Heat Capacity of 1-Butene and 1-Pentene at Bubble Point

III. Mass Transfer in a Turbulent Air Stream

Thesis by

Warren Gleason Schlinger

In Partial Fulfillment of the Requirements

for the degree of

Doctor of Philosophy

California Institute of Technology
Pasadena, California
1949

Acknowledgment

The help and guidance of Professor B. H. Sage made possible the design work and experimental studies reported in this thesis. The author is indebted to Hollis H. Reamer and many other persons associated with the Chemical Engineering Laboratory who have contributed materially to the construction and operation of the volumetric apparatus described in Part I. The aid of Robert E. Sears and Lawson G. Smith in the design of the equipment and the assistance of Willard D. DeWitt who machined the major parts of the apparatus are gratefully acknowledged. Bert H. Golding contributed greatly to the construction of the equipment. Separate acknowledgments have been included with Parts II and III which have been prepared in manuscript form for publication under the joint authorship of W. G. Schlinger and B. H. Sage.

Abstract

Part I

An apparatus was designed and constructed to determine the volumetric behavior of a number of corrosive fluids at pressures up to 10,000 pounds per square inch and temperatures ranging from -30° to 360°F. Photographic illustrations of the equipment are included and the operation and calibration procedures discussed. Some measurements of the volumetric behavior of nitrogen dioxide are presented in graphical and tabular form.

Part II

The isobaric heat capacity at bubble point of 1-butene and 1-pentene was determined at temperatures from 90 to 200°F. These measurements were carried out in the two-phase region in a constant-volume adiabatic calorimeter. The isobaric heat capacity at bubble point was calculated from the directly measured isochoric values by the use of supplementary volumetric data. The latter data were obtained experimentally for 1-butene and were estimated from the law of corresponding states for 1-pentene. The results are presented in graphical and tabular form.

Part III

Values of the eddy diffusivity were determined for turbulently flowing coaxial streams of natural gas and air. The primary

measurements included the composition and velocity as a function of radial position and distance from the point at which mixing of the coaxial streams began. The investigations were carried out at gross velocities of 25, 50, and 100 feet per second in a working section 4 inches in diameter and 8 feet in length. The air and natural gas entered the working section at substantially the same relative gross velocities in the case of each set of measurements. Experimental results and derived values of the eddy diffusivity are presented and a method of predicting the composition pattern is discussed.

Table of Contents

Part II. (Cont'd)

Part III. Mass Transfer in a Turbulent Air Stream

Part I

An Apparatus to Determine the Volumetric Behavior of Oxides of Nitrogen

Introduction

Under an Office of Naval Research contract the Chemical Engineering Laboratory of the California Institute of Technology is studying the thermodynamic properties of nitrogen dioxide and its mixtures with nitric oxide. These studies extend to higher pressures and temperatures than have heretofore been reported in the literature. The equipment necessary to establish the volumetric behavior of the oxides of nitrogen has been designed and constructed and some measurements of the properties of nitrogen dioxide made.

Previous studies (1) indicated that the rate of reaction of thoroughly dehydrated nitrogen dioxide and mercury was high at room temperature. Therefore, it was not feasible to use mercury as a confining fluid in the volumetric apparatus. Since no suitable liquid substitute for mercury was found, the construction of an apparatus with a variable volume cell was impractical and a bomb or working section of constant volume was designed. The following portion of Part I of the thesis describes in detail the design and construction of equipment suitable for determining the volumetric behavior of a number of corrosive fluids over a range of pressures from 20 to 10,000 pounds per square inch absolute and temperatures from -30° to 360°F.

The essential features of the apparatus include a stainless steel spherical working section immersed in a thermally regulated silicone* bath, instruments necessary for the precision measurement and control of temperature, and a thin diaphragm and associated assembly through which pressures are transmitted to a fluid pressure balance. The major part of the equipment is mounted in a steel structure providing adequate

* Silicone (type LT-NV20) was obtained from the General Electric Corporation and employed over the entire temperature range.

protection to the operator. The temperature measurement and control instruments are housed separately in an adjacent structure.

Working Section

The stainless steel working section was machined from a solid forging of type 302 stainless steel to form two threaded hemispherical sections which are shown prior to assembly in Figure 1. The interior of the working section which is 5 inches in diameter has a polished surface. In general, the wall of the cell is 1/2 inch in thickness except in the vicinity of the threaded section where it is enlarged to a maximum of 3/4 inch to allow for the somewhat higher stresses induced by the threads. A buttress thread with a 1-degree taper was machined on each of the hemispherical sections in order to insure a thread of maximum strength and to form a seal when the cell is assembled. In addition a thin tapered lip approximately 1/4 inch high and varying in thickness from 0.020 to 0.004 inch was formed on a male section. This lip engages the female section upon assembly and provides a semi self-sealing joint. The tapered buttress thread and thin lip may be seen in Figure 1. Before final assembly the threaded portion of each half and the lip were carefully tinned with a solder containing 97 weight per cent tin and 3 weight per cent lead. A slight excess of solder was left on the threads and the two halves were assembled while the solder was molten.

Two small threaded bosses 7/8 inch wide and 5/8 inch high were machined on an axis and as an integral part of the working section. These bosses which are shown in Figure 1 serve as a means for mounting the cell

within the thermally controlled silicone bath. On another diameter of the working section perpendicular to the mounting bosses, housings are machined for two valves through which material may be added to the interior of the bomb. The valve housings may be seen in the photographs of the assembled cell shown in Figures 2 and 3.

Pressure Measurements

A boss approximately 2 1/4 inches in diameter and extending 1 inch above the spherical surface was machined on the working section. This boss contains the thin diaphragm mechanism required for the establishment of pressures existing within the cell. The diaphragm assembly consists of a stainless steel disc 1.5 inches in diameter and 0.010 inch in thickness soldered onto a hollowed plug which fits into the boss on the bomb. The plug is secured in the boss by a split nut which bears on a lead gasket forming an unsupported-area seal. The center of the thin circular disc or diaphragm has an unrestrained movement of approximately 0.007 inch in either direction from its equilibrium position before the disc makes contact with a surface which was machined to conform with the elastic deformation produced in the diaphragm during the small movement from its equilibrium setting. These machined backings prevent any permanent deformation of the diaphragm due to large pressure differences occurring across the thin disc.

There is a small pin in the center of the diaphragm which makes contact with the lower portion of a spring-supported and electrically-insulated surface when a small pressure differential exists across the

diaphragm. This electrical contact, which carries a current of approximately 30 miscroamperes, serves to establish a reproducible pseudoequilibrium position of the diaphragm. The movement of the diaphragm is accomplished by varying the pressure of a hydraulic silicone which is confined on the outer side of the diaphragm. The electrical circuit is lead to the top of the diaphragm housing and through a crushed, partially dehydrated soapstone seal which effectively insulates the electrical lead yet seals the system at all pressures throughout the temperature range. The small current flowing through the contact is amplified by an electronic circuit and operates a neon light.

To measure the pressure existing in the working section, silicone is introduced by means of a hand-operated injector into the chamber behind the diaphragm. When sufficient fluid is injected or removed the neon light indicates the diaphragm is in its equilibrium position. Photographs of the assembled and disassembled injector constitute Figures 4 and 5. The pressure in the silicone-filled part of the system is transmitted through a mercury trap or U-tube to a line containing a hydraulic oil. The pressure in this oil line is measured with a fluid pressure balance. The pressure in the oil line is adjusted manually by an injector of the type shown in Figure 5.

Temperature Measurement and Control

In order to establish the temperature existing within the working section it is assumed that the measured temperature of the silicone

bath is equal to that of the material confined in the cell. The attainment of thermal equilibrium within the spherical bomb is indicated by the constancy with respect to time of the pressure which is measured with the diaphragm pressure gauge. The silicone in the bath and the material in the working section are thoroughly agitated to hasten the approach to equilibrium. The agitation of the material within this section is accomplished by means of an oscillatory motion imparted to the spherical cell. This movement which rotates the working section through 180 degrees with a period of about 1 second is accomplished by the mechanism shown partially assembled in Figure 6. This assembly, which is activated by a small electric motor, may also be seen in its mounted position in Figure 10. The silicone in which the working section is immersed is thoroughly agitated by an impeller located in the bottom of the bath. The impeller is shown before assembly in the apparatus in Figure 7. A suitable baffle is placed within the bath so as to provide adequate circulation of the silicone set in motion by the impeller. The interior of the silicone bath, the baffle, the top of the impeller, the spherical working section, and the housing for the diaphragm pressure gauge are shown in their mounted positions in Figure 8.

The silicone bath which has a capacity of approximately 10 gallons is thermally regulated by a droop-corrected thyratron (2) control circuit capable of supplying up to 500 watts of control energy. An adequate heat transfer rate is provided from the silicone bath to the controlling elements so that the temperature may be controlled

within 0.001°F of a predetermined value within the range of operation. The controlling electrical energy necessary for the fine temperature adjustment is added to the bath through a bare resistance heater immersed in the bath. The location of the heating element may be seen in Figure 8. The temperature of the bath is measured with a strain-free platinum resistance thermometer and a precision-type Mueller resistance bridge.

The silicone bath is encircled by a 50-foot length of 3/8-inch copper tubing through which chilled silicone may be circulated. Thermal energy is removed from this circulating fluid in a heat interchanger supplied with Freon-12. The circulating silicone may be cooled to -40°F thus permitting the bath to be operated at temperatures as low as -30°F. In addition to the coils of copper tubing the outer surface of the silicone bath is equipped with electrical heaters capable of supplying 1700 watts. These high-wattage heating elements are used for providing rapid changes in the bath temperature.

The silicone bath is surrounded by a radiation shield which is mounted so as to leave an air space of approximately 1 inch. This outer shield is supplied with refrigeration coils and is equipped with electrical resistance heating elements which, coupled with variable voltage transformers, supply a maximum of 3500 watts. The heating elements are divided into four sections: the bottom, the lower side, the upper side, and the top of the shield. With this arrangement of heating elements it is possible to control the temperature of the inner surface of the

radiation shield to a predetermined value. This control prevents excessive thermal losses from the inner bath and enables the attainment of a more uniform temperature within the agitated silicone. The loss of thermal energy from the bath through the shaft which drives the impeller and the shaft which oscillates the working section is prevented by the adjustment of the electrical input to small-wattage heating elements located on the surface of these shafts where they protrude through the radiation shield. In order to establish the desired rate of heat input to the various sections of the shield, thermocouples are placed on the inner surface and a measurement is made of the differential electromotive force produced between this junction and a junction immersed in a well in the silicone bath.

The silicone in the cooling systems is circulated by small gear pumps driven by fractional-horsepower motors. Separate systems are provided for the circulation of chilled silicone around the bath and the radiation shield. For rapid changes in temperature both sets of cooling coils may be employed. However, once the lower desired temperature is attained the circulation of the silicone in the cooling coils on the bath is stopped. This technique greatly facilitates the accurate control of temperature within the bath when there are minor fluctuations in the supply and intake pressures of the refrigeration system. The heat interchanger and part of the circulating system may be seen in Figure 10.

A reservoir is provided to allow for the change in volume of the silicone accompanying changes in the temperature of the bath. The

excess silicone which accumulates because of thermal expansion returns to the reservoir through an overflow line and may be replaced in the bath when the temperature is lowered. The reservoir, which may be seen in the lower left corner of Figure 10, is large enough to hold the entire quantity of silicone within the bath if the removal of the fluid is necessary for repair operations.

Sample Addition

Material may be added to the working section through either or both of the two valves which are located on opposite sides of the spherical cell. The sample is conducted to each valve through a length of type 302 stainless steel hypodermic tubing having an inside diameter of 0.020 inch. The two tubing lines together with the similar piece of tubing which leads to the diaphragm pressure measuring assembly are wound in a helix before being attached to the working section. This helix permits the bomb to be oscillated without damaging the stainless steel tubing. The two sampling tubes terminate on the exterior of the equipment in a small valve manifold which permits material to be added to the cell by standard weighing bomb techniques (2). This manifold also allows the tubing lines to be connected to a high-vacuum system in order to evacuate the bomb.

The valves which are located on the surface of the bomb permit the sample to be entirely isolated in the bomb and it is unnecessary to make any corrections for the amount of sample retained in dead spaces

or any associated part of the equipment which is not adequately thermostated. Cooling the cell or heating the weighing bomb facilitates the addition of condensable materials to the cell. When the valve on the surface of the cell is closed, any material remaining in the hypodermic tubing lines is removed by recondensing the sample using liquid air or other suitable coolant on the surface of the weighing bomb. One of the loading valves on the working section and some of the hypodermic tubing leads are depicted in Figure 8.

Equipment Housing

The equipment necessary to determine the volumetric behavior of corrosive fluids is housed in a steel and aluminum structure approximately 7 feet square and 6 feet high. The housing is divided into three sections which are shown in the early stages of construction in Figure 9. One section, which is approximately 3 feet square and located 3 feet above the floor level, is surrounded on four sides and on the bottom by pieces of 1/2-inch hot-rolled steel plate. This cubical framework contains the silicone bath, the radiation shield, and the actual working section. An overhead view of this portion of the apparatus is presented in Figure 8. In this figure the spherical cell may be seen in its mounted position. This photograph also shows the silicone bath, the insulated radiation shield, and a portion of the refrigerating tubing.

An appropriate housing which is approximately 4 feet wide and 7 feet long is provided for the associated pieces of apparatus which are

necessary for the operation of the equipment. A view of the interior of this housing comprises Figure 10. In this photograph the mechanism which oscillates the working section may be seen in its mounted position, the displacement cylinders used in connection with pressure measurements are shown, and the Freon-silicone heat interchanger together with its associated gear pumps for circulating the chilled silicone is depicted. The third section of the equipment consisting of a space approximately 3 feet square is reserved for housing any unforeseen additions to the apparatus.

The exterior of the equipment housing is shown before completion in Figure 11. This figure shows the location of the displacement cylinders and associated pressure gauges, the valves and gauges connected with the refrigeration system, and the controls necessary for the transfer of the silicone to and from the bath. The figure also shows the location of the radiation shield with two of the protective steel plates removed.

In addition to the housing described above a separate structure has been built to contain the instruments required for the measurement and control of temperature. A photograph of this housing constitutes Figure 12 and shows the location of the precision-type Mueller bridge necessary for the measurement of the temperature, the decade box and ammeters associated with the droop temperature control circuit, and a student-type potentiometer employed in electromotive force measurements of the thermocouples. This temperature control housing is of a universal character.

All the leads from the apparatus are brought to the terminal connections or jacks shown in Figure 12 and by means of jumpers a given instrument may be connected to the desired outlet terminals. The interior of this housing is depicted in Figure 13 before the wiring was installed. The relative position of the temperature control housing and the volumetric apparatus is presented in Figure 14. This photograph shows the location of a portion of the electrical controls of the volumetric equipment.

Calibration

The primary measurements made with the apparatus are the weight of the sample, pressure, temperature, and a nearly constant total volume. Temperature is measured with a strain-free platinum resistance thermometer and a precision-type Mueller bridge. The Mueller bridge was calibrated with standard resistances bearing certificates issued by the Bureau of Standards. The calibration was conducted at three temperatures to determine the temperature coefficients of bridge coils. The experimentally determined coefficients are in good agreement with published values (3) for manganin resistance coils. The calibration of the bridge enables the absolute resistance of the platinum thermometer to be determined with a probable error of 0.0004 ohm.

The resistance of the measuring thermometer at a fixed temperature was compared with that of a similar instrument* which had been certified by the Bureau of Standards. This comparison was conducted at a

---

* Leeds and Northrup No. 8163

sufficient number of points that the application of the Callendar equation (4) enables the temperature of the fluid bath to be established with an uncertainty of less than 0.04°F relative to the international platinum scale.

The pressure within the working section as measured with a fluid pressure balance (2) must be corrected for several factors. One factor referred to as "A" involves the gauge constant of the pressure balance. This factor is determined by periodically measuring the known vapor pressure of carefully purified carbon dioxide at the ice point.

Since the pseudoequilibrium position of the thin diaphragm does not necessarily correspond to a position where the pressure on either side is equal, a second correction factor is considered. This pressure differential, together with a pressure correction due to the difference in elevation between the diaphragm and the pressure balance, is termed the "B" constant of the apparatus. This constant changes with temperature since this variable affects the pseudoequilibrium position of the diaphragm as well as the density of the hydraulic fluid in the oil lines. The "B" constant was determined by filling the working section to a known pressure conveniently measured with a mercury manometer and a vertical component cathetometer. Measuring the pressure with the balance suffices to determine the "B" constant. This calibration is carried out at several temperatures and gives a quantity which must be added to all measured pressures. Thus, to establish the pressure existing in the working section the following equation is applicable:

$$P = R_t A + B + P_a \qquad (1)$$

The magnitude of the "B" constant as a function of temperature is shown in Figure 15. From considerations of the design of the diaphragm pressure gauge it is assumed that the "B" constant does not change with pressure. However, it is suggested that this assumption be verified by measuring the vapor pressure of carbon dioxide at the ice point and by comparing the resulting value of "B" obtained by the use of equation (1) and the independently established "A" calibration of the pressure balance.

Two methods were employed to determine the volume of the working section. In the first method air was displaced into the evacuated bomb by a weighed quantity of mercury. The air and the working section were maintained at the same temperature. Pressure measurements made with a cathetometer and a mercury manometer before and after displacement sufficed to establish the volume of the working section.

In the second method the bomb was filled with pure methane to a pressure of approximately 1000 pounds per square inch. After accurately establishing the pressure and temperature in the working section, a sample of methane was withdrawn and weighed. This information together with a knowledge of the pressure and temperature in the bomb after the sample withdrawal enables the volume to be computed. Published data concerning the volumetric behavior of methane (5,6) were employed. This withdrawal procedure, which was repeated several times, provided sufficient data to

establish accurately the volume of the cell. The variation of the volume of the working section with pressure and temperature was established from information concerning the value of Young's modulus and the coefficient of thermal expansion. The total volume of the working section in cubic feet is given by the following expression:

$$V = 0.033694(1 + 2.7\times10^{-5}t + 2.0\times10^{-7}P) \qquad (2)$$

in which P is the pressure in pounds per square inch absolute and t the temperature in $^{\circ}$F. The two methods of measurement established the volume of the working section with an estimated uncertainty of 0.1 per cent.

Experimental Measurements

A limited number of measurements were made on the volumetric behavior of nitrogen dioxide. These measurements included the determination of pressure as a function of the temperature of the sample confined in the spherical working section. The studies were conducted in temperature intervals of 20 degrees ranging from 100° to 340°F and were made with three different masses of material in the working section.

The nitrogen dioxide, obtained from a commercial source* was purified by partial condensation at -90°F and fractionation at atmospheric pressure. Before condensation the gaseous sample was conducted through driers containing anhydrous calcium sulfate and phosphorous pentoxide. High-vacuum techniques were employed throughout the purification process.

* E. I. du Pont de Nemours & Co. (Inc.), Wilmington, Delaware

Several pressure determinations were made in the two-phase region. These results are presented in Table I and are shown graphically on a residual basis in Figure 16. The vapor pressure of nitrogen dioxide has been reported by Sheffer (7), Baume (8), and Mittasch (9). Only the studies of Sheffer extended to temperatures above 120°F. The experimental values of Sheffer and Mittasch are also indicated in Figure 16. The vapor pressures measured in the present investigation at low temperatures are higher than the values reported previously. This variation may be caused by differences in sample purity since Smits (10) has shown that the vapor pressure of nitrogen dioxide at room temperature increases 0.5 pound per square inch when the last traces of water are removed from the sample. Smits indicates that this variation is caused by the effect of small traces of water vapor on the dissociation equilibrium.

The information obtained in the one-phase gaseous region with the three quantities of material in the working section is presented in Table II. These data while very limited are believed to have an uncertainty of less than 0.3 per cent. Table II includes the value of the compressibility factor defined by equation (3)

$$Z = \frac{PV}{bT} \tag{3}$$

in which the specific gas constant b is equal to R/M. The molecular weight of NO_2 was taken as 46.008 based on atomic weights of 1942.

Nomenclature

A pressure calibration factor, dimensionless

B pressure calibration factor, lb/sq.in.

b specific gas constant, (cu.ft/lb)(lb/sq.in.)/^{o}R

M molecular weight

R universal gas constant = 10.73185, (cu.ft/mole)(lb/sq.in.)/^{o}R

P pressure, lb/sq.in. abs

T temperature, ^{o}Rankine

t temperature, ^{o}Fahrenheit

$\underline{V}$ total volume, cu.ft

V specific volume, cu.ft/lb

Z compressibility factor, dimensionless

Subscripts

a refers to atmosphere

b refers to pressure balance

References

(1) Pierce, W. C., Noyes, W. A., Jr., J. Am. Chem. Soc., 50, 2179 (1928).

(2) Sage, B. H. and Lacey, W. N., Trans. Am. Inst. Mining Met. Engrs., 136, 136 (1940).

(3) American Institute of Physics, Temperature--Its Measurement and Control in Science and Industry, Reinhold Publishing Company, p 162 (1941).

(4) Callendar, H. L., Phil. Trans., London, 178, 160 (1887).

(5) Michels, A. and Nederbragt, G. W., Physica, 3, 569 (1936).

(6) Olds, R. H., Reamer, H. H., Sage, B. H., and Lacey, W. N., Ind. Eng. Chem., 35, 922 (1943).

(7) Sheffer, F. E. C. and Treub, J. P., Zeit. fur Phys. Chem., 81, 308 (1912).

(8) Baume, G. and Robert, M., Comp. Rend. 168, 1199 (1919).

(9) Mittasch, A., Kuss, E., and Schlueter, H., Zeit. Anorg. Allgem. Chem., 159, 1 (1926).

(10) Smits, A., de Liefde, W., Swart, E., and Claassen, A., J. Chem. Soc., London, 129, 2657 (1926).

Table I. Vapor Pressure of Nitrogen Dioxide

Temp. °F	Vapor Pressure lb/sq.in.abs
100	31.45
120	49.23
140	75.28
160	112.15
180	163.73
200	235.14
220	331.12

Table II. Volumetric Properties of Nitrogen Dioxide

Temp. °F	Pressure lb/sq.in. abs	Specific Volume cu.ft/lb	Compressibility Factor*
200	208.4	0.4587	0.6211
	229.1	0.3901	0.5809
220	230.8	0.4590	0.6682
	261.3	0.3903	0.6433
240	253.8	0.4592	0.7141
	288.9	0.3905	0.6912
	458.6	0.1746	0.4906
260	276.6	0.4594	0.7570
	316.8	0.3907	0.7373
	567.0	0.1747	0.5900
280	300.1	0.4597	0.7996
	344.3	0.3909	0.7801
	632.0	0.1748	0.6402
300	321.9	0.4599	0.8356
	371.0	0.3912	0.8189
	697.3	0.1749	0.6881
320	342.6	0.4602	0.8669
	396.0	0.3914	0.8521
	761.4	0.1750	0.7326
340	361.8	0.4604	0.8930
	419.3	0.3916	0.8802
	824.3	0.1751	0.7737

* See equation (3)

Figure 1. Disassembled Working Section

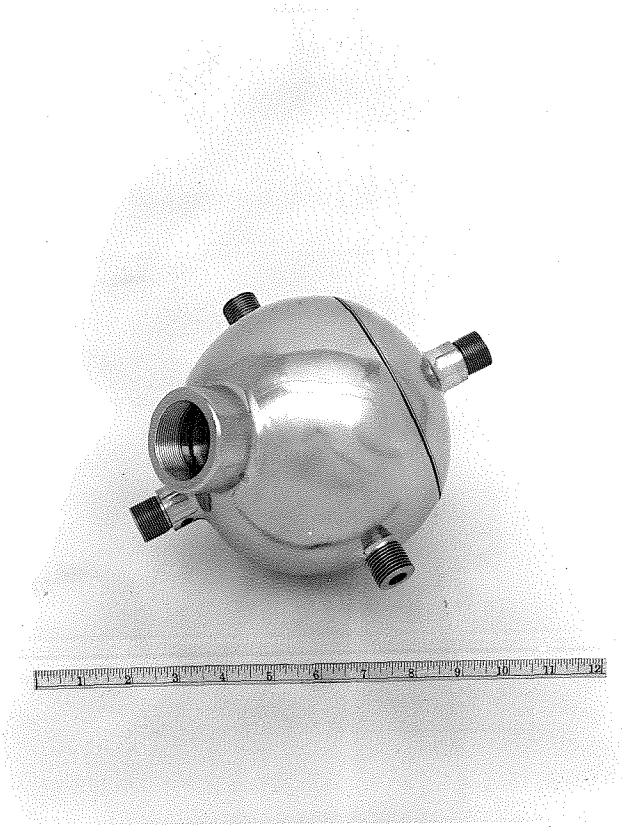

Figure 2. Assembled Working Section

Figure 3. Assembled Working Section

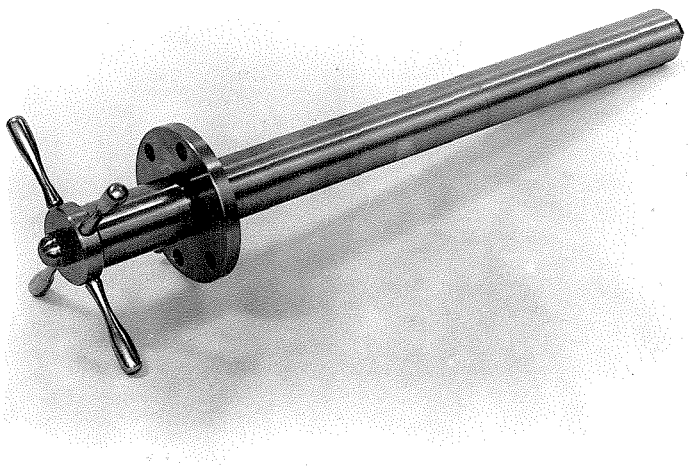

Figure 4. Hand-Operated Injector

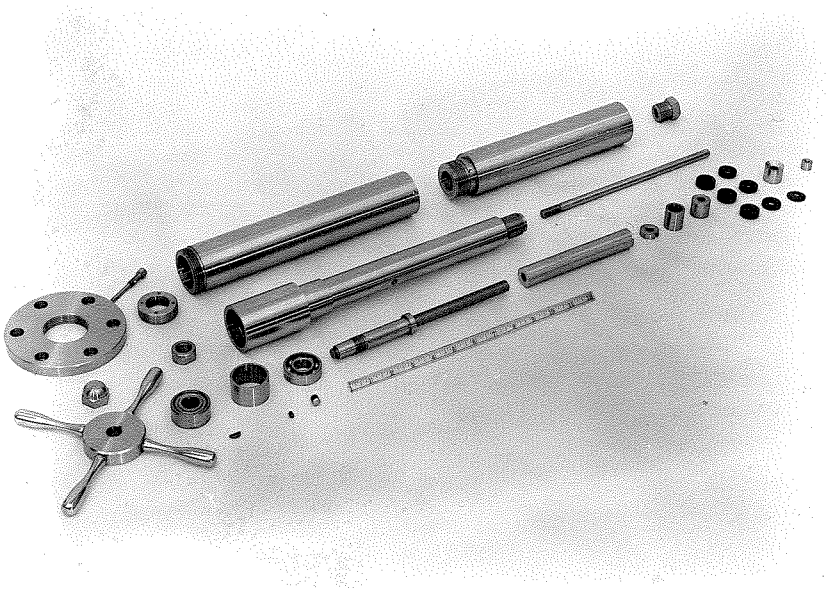

Figure 5. Disassembled Injector

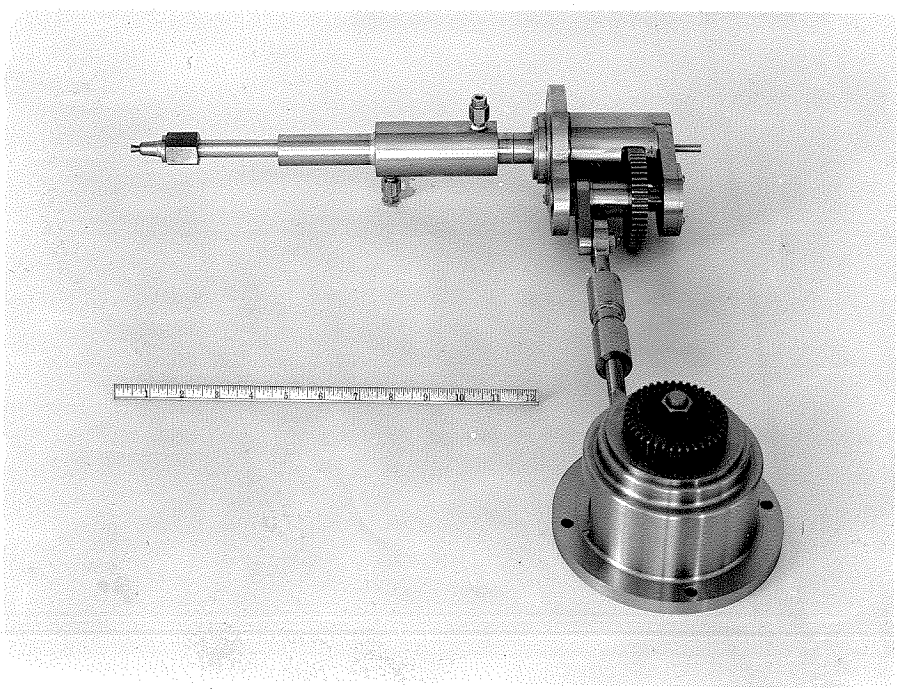

Figure 6. Agitation Assembly

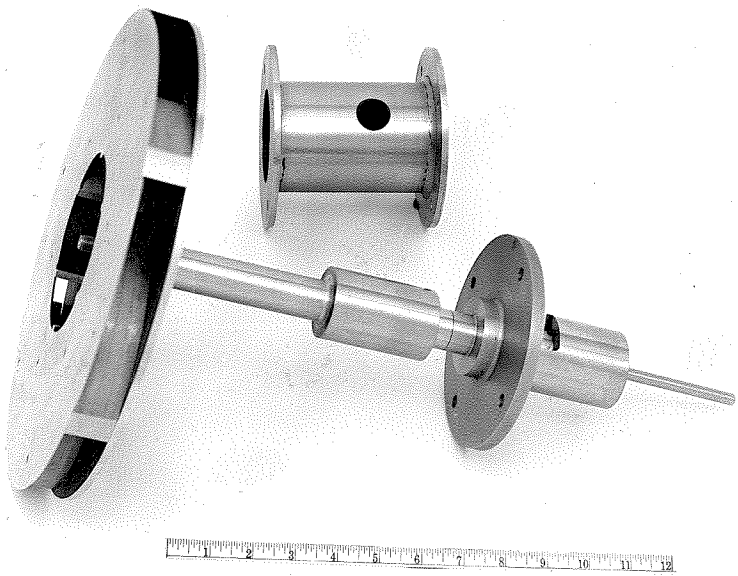

Figure 7. Impeller Assembly

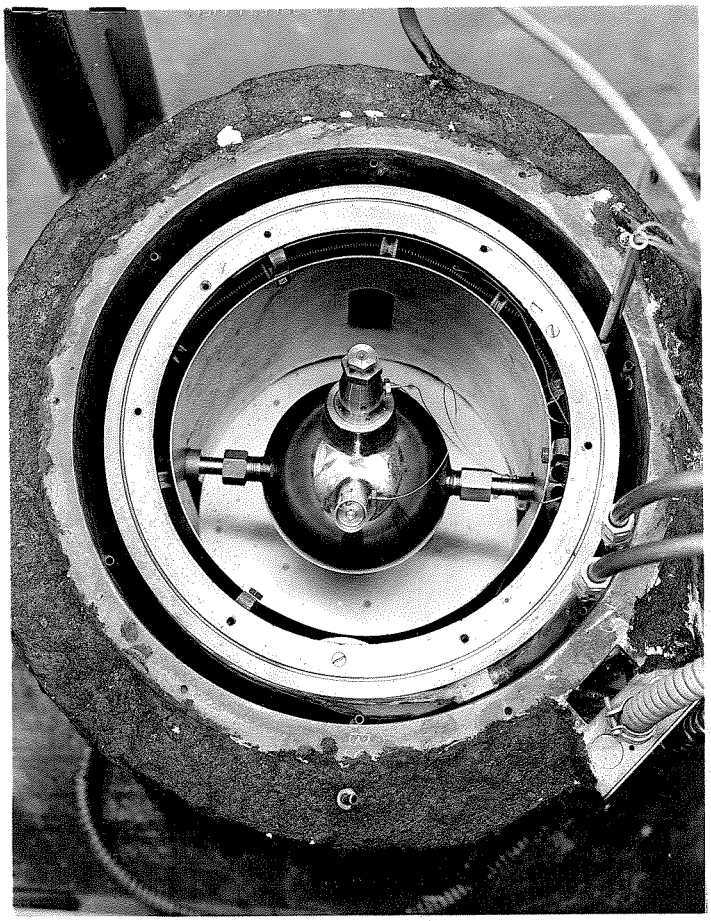

Figure 8. Overhead View of the Silicone Bath

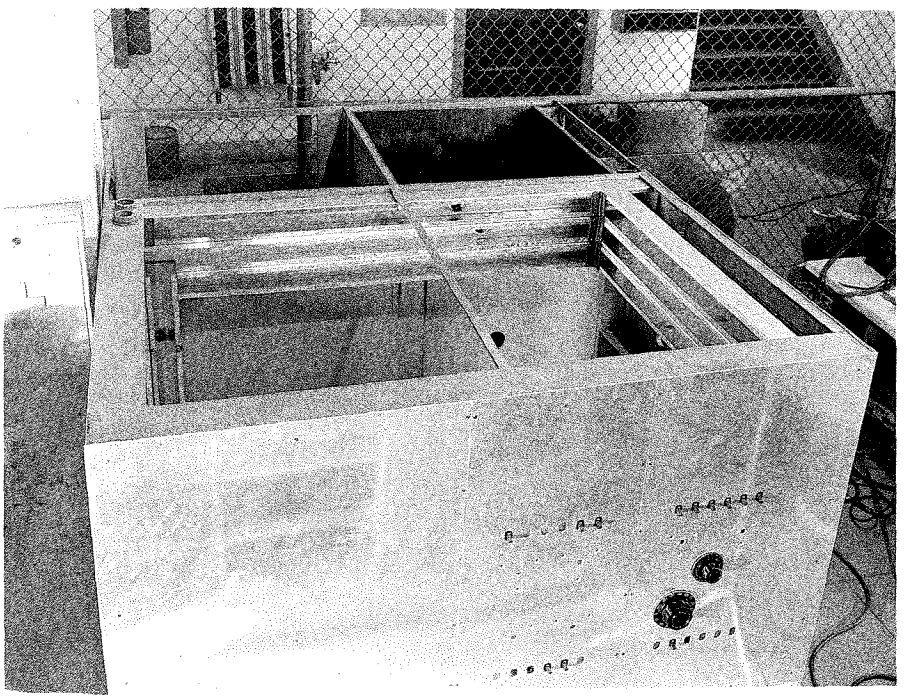

Figure 9. Top View of the Equipment Housing

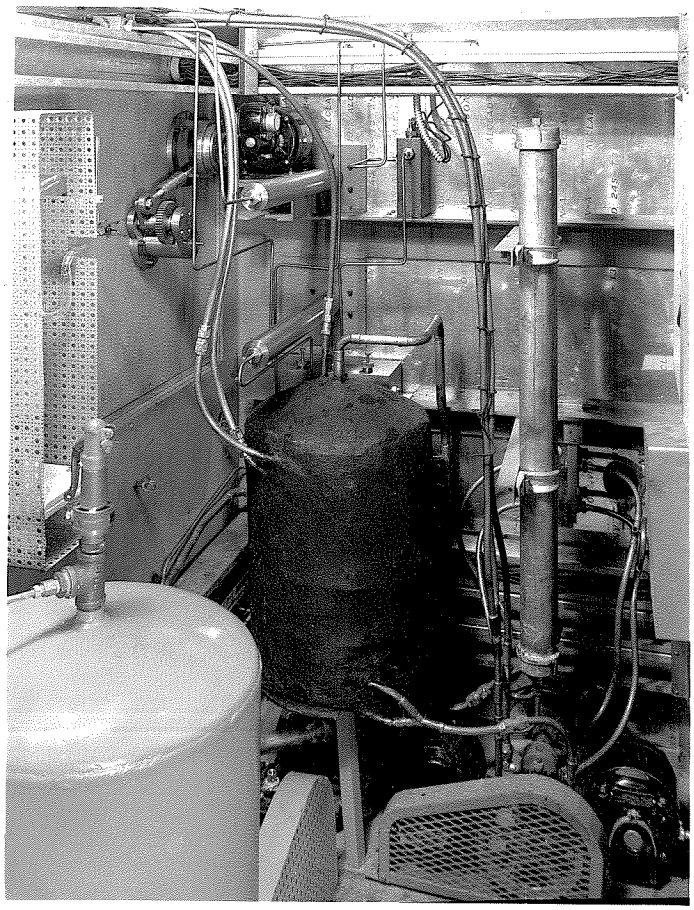

Figure 10. Interior of the Equipment Housing

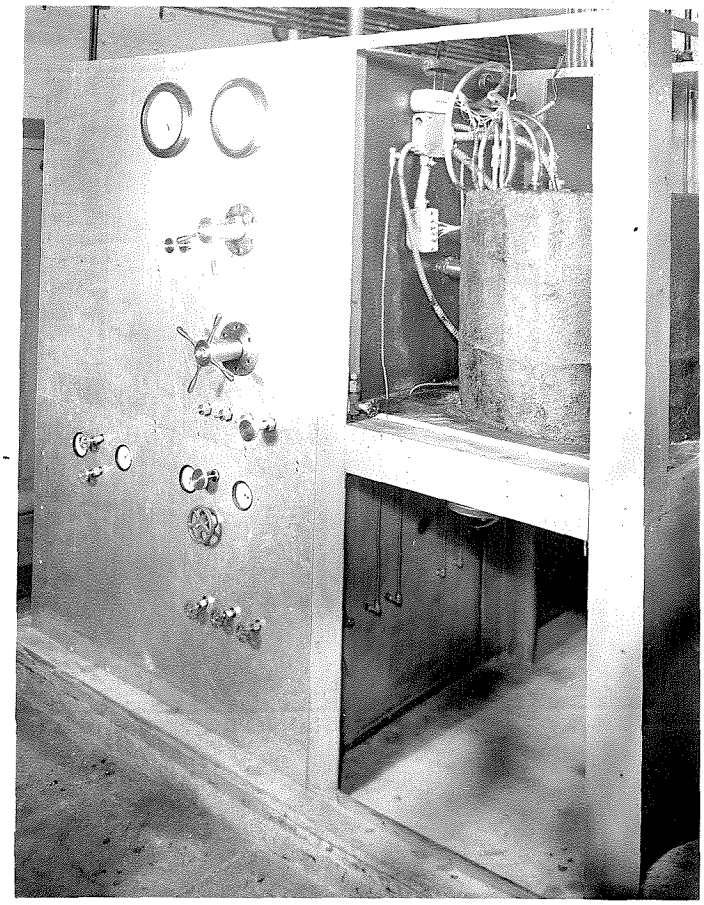

Figure 11. Exterior of the Equipment Housing

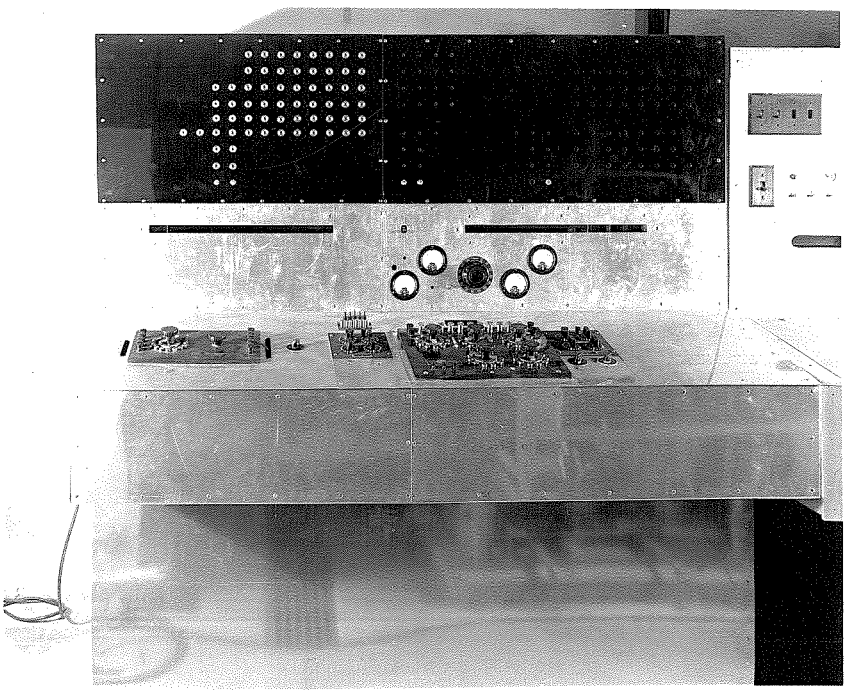

Figure 12. Exterior of the Temperature Control Housing

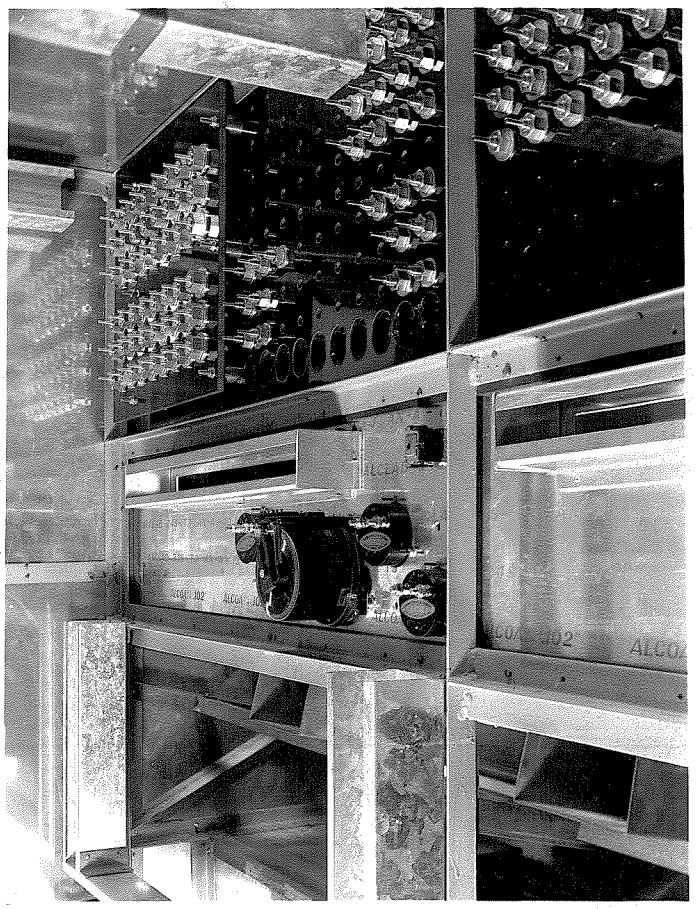

Figure 13. Interior of the Temperature Control Housing Prior to Installation of Wiring

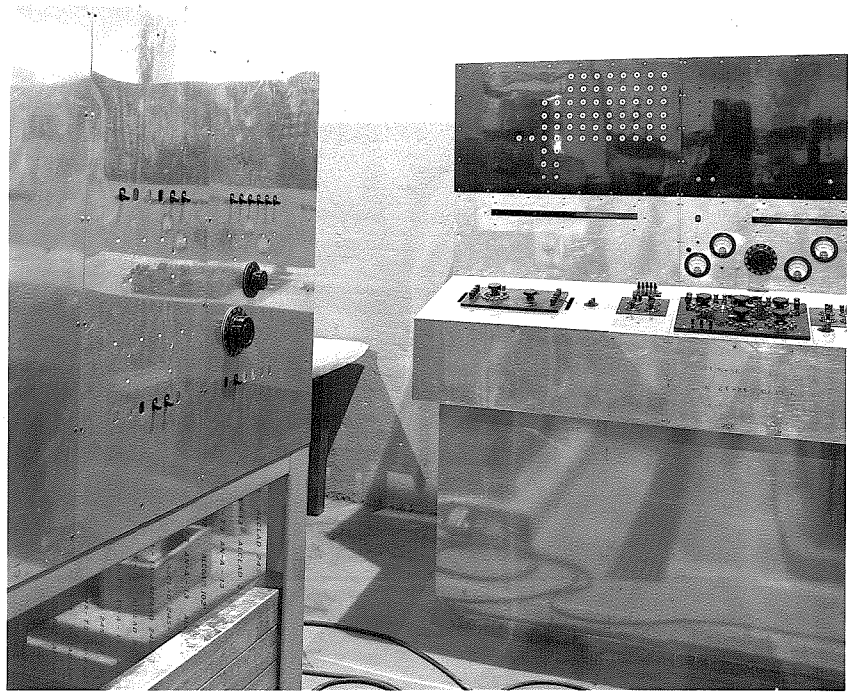

Figure 14. Relative Location of the Equipment Housings

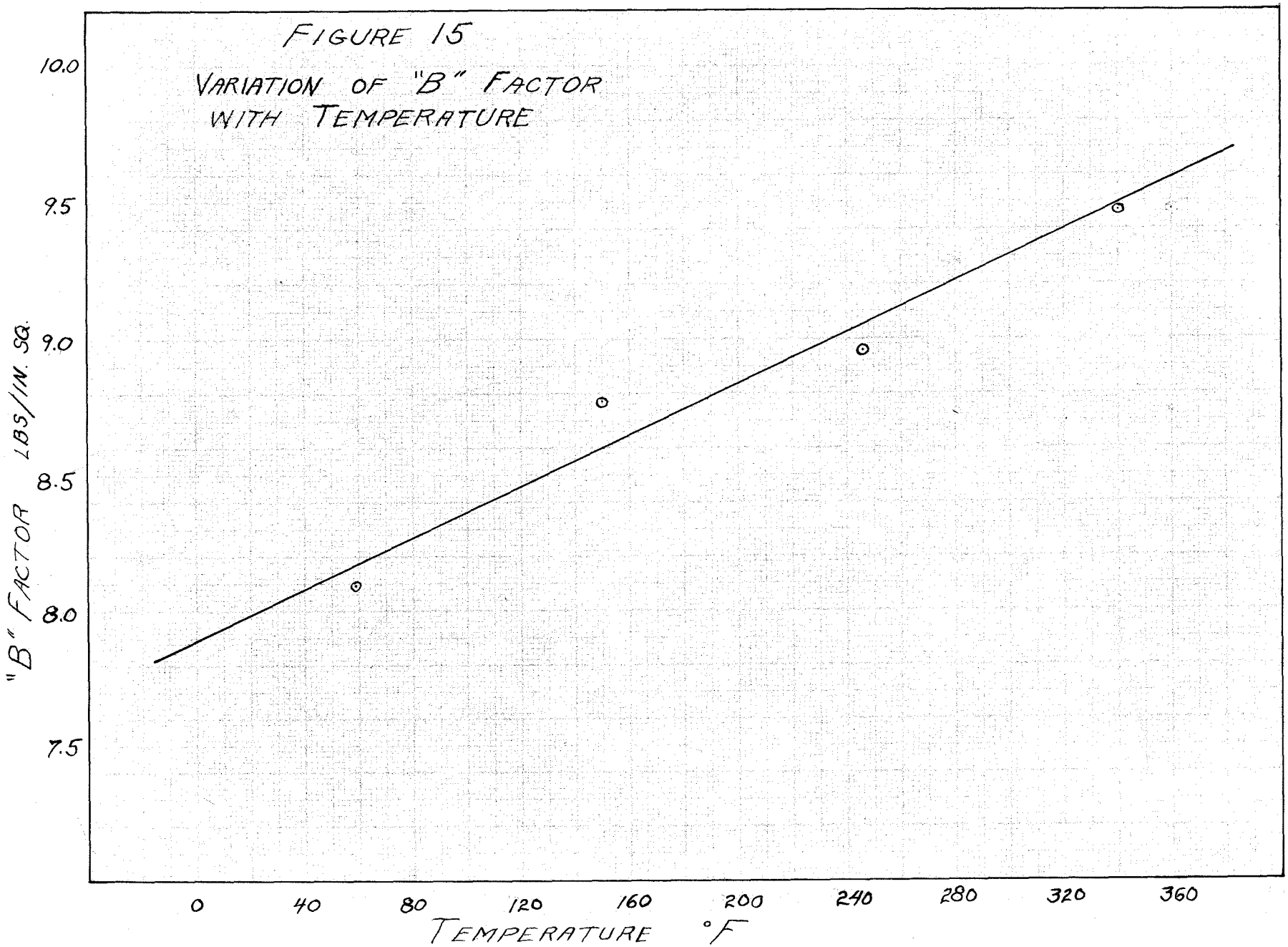
FIGURE 15
VARIATION OF "B" FACTOR WITH TEMPERATURE
10.0
9.5
9.0
8.5
8.0
7.5
"B" FACTOR LBS/IN. SQ.
0
40
80
120
160
200
240
280
320
360
TEMPERATURE °F

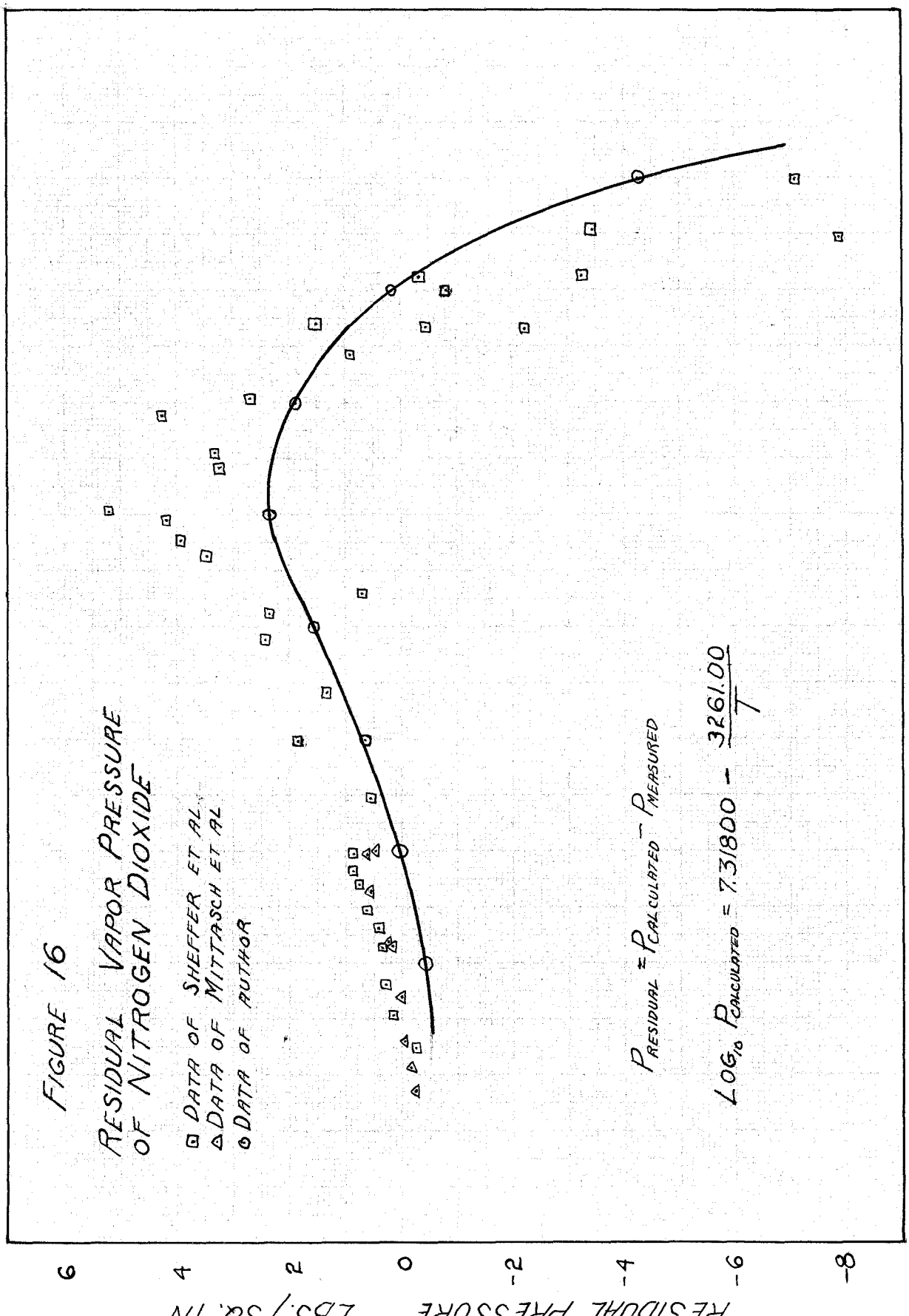
FIGURE 16
RESIDUAL VAPOR PRESSURE OF NITROGEN DIOXIDE
□ DATA OF SHEFFER ET AL.
△ DATA OF MITTASCH ET AL
○ DATA OF AUTHOR
$P_{RESIDUAL} = P_{CALCULATED} - P_{MEASURED}$
$LOG_{10} P_{CALCULATED} = 7.31800 - \frac{3261.00}{T}$
RESIDUAL PRESSURE LBS./SQ. IN
6
4
2
0
-2
-4
-6
-8
80
100
120
140
160
180
200
220
240
TEMPERATURE °F

Part II

Isobaric Heat Capacity of 1-Butene and 1-Pentene at Bubble Point

Introduction

The information available concerning the heat capacity of 1-butene and 1-pentene in the liquid phase is limited to measurements at temperatures below 70°F. Aston et al (1) presented heat capacities for liquid 1-butene at temperatures from 20° to 470° Rankine. Huffman and co-workers (2) carried out measurements upon the heat capacity of liquid 1-pentene in the temperature interval between 20° and 530° Rankine. As a result of the absence of such data at the high temperatures, an investigation of the isobaric heat capacity of bubble-point liquid for 1-butene and 1-pentene has been carried out.

The measurements were made in the two-phase region utilizing a constant-volume calorimeter. In order that the directly measured information involving the energy required to heat the calorimeter bomb and contents through a predetermined temperature interval could be resolved into the isobaric heat capacity at bubble point, a thermodynamic analysis of the process was required. The calorimetric measurements were carried out with at least two different quantities of the pure hydrocarbon in the calorimeter. It can be shown from a consideration of a material balance and the first law of thermodynamics that for any two-phase, one-component system the following equation applies:

$$dE = m_d\left[\left(C_{P,d} - P\left(\frac{\partial V}{\partial T}\right)_{P,d}\right)dT + \left(\ell_{P,d} - P\left(\frac{\partial V}{\partial P}\right)_{T,d}\right)dP\right]$$

$$+(m-m_d)\left[\left(C_{P,b} - P\left(\frac{\partial V}{\partial T}\right)_{P,b}\right)dT + \left(\ell_{P,b} - P\left(\frac{\partial V}{\partial P}\right)_{T,b}\right)dP\right] \qquad (1)$$

$$+ (E_d - E_b)\,dm_d$$

Considering the second law and applying equation (1) to two different quantities of material in the bomb at the same temperature there is obtained

$$\underline{\mathcal{E}}_1 - \underline{\mathcal{E}}_2 = (m_{d_1} - m_{d_2})\left[C_{P,d}\,dT - P\,dV_d - T\left(\frac{\partial V}{\partial T}\right)_{P,d} dP\right]$$

$$+ (m_1 - m_2 + m_{d_1} - m_{d_2})\left[C_{P,b}\,dT - P\,dV_b - T\left(\frac{\partial V}{\partial T}\right)_{P,b} dP\right] \qquad (2)$$

$$+ \left(T\frac{dP''}{dT} - P\right)(V_d - V_b)(dm_{d_1} - dm_{d_2})$$

Expressing $(dm_{d_1} - dm_{d_2})$ and $(m_{d_1} - m_{d_2})$ in terms of V_b, V_d and $(m_1 - m_2)$ the following useful equation results, which applies to the processes in question:

$$C_{P,b} = \frac{\frac{\underline{\mathcal{E}}_1}{dT} - \frac{\underline{\mathcal{E}}_2}{dT}}{m_1 - m_2}\left(\frac{V_d - V_b}{V_d}\right) + T\left(\frac{\partial V}{\partial T}\right)_{P,b}\frac{dP''}{dT}$$

$$+ T\left(\frac{dP''}{dT}\right)\left(\frac{V_d\frac{dV_b}{dT} - V_b\frac{dV_d}{dT}}{V_d}\right) + \frac{V_b}{V_d}\left[C_{P,d} - T\left(\frac{\partial V}{\partial T}\right)_{P,d}\frac{dP''}{dT}\right] \qquad (3)$$

Equation (3) required certain volumetric data concerning the material in question and includes the isobaric heat capacity of the dew-point gas.

The thermal quantities in equation (3) $\frac{\mathcal{E}_1}{dT}$ and $\frac{\mathcal{E}_2}{dT}$ represent the net electrical energy required per unit temperature change of the calorimeter bomb and its contents. These thermal quantities must be corrected for the thermal losses from the calorimeter and for the energy added in the course of the agitation of the contents of the calorimeter. Equation (3) indicates that the influence of the heat capacity of the dew-point gas on the heat capacity of the bubble-point liquid is relatively small. This results from the fact that the ratio of the specific volume of the bubble-point liquid to that of the dew-point gas is small except in the vicinity of the critical state. For this reason, relatively large uncertainties in the isobaric heat capacity and in the isobaric volume-temperature derivative for dew-point gas do not influence appreciably the resultant values of the isobaric heat capacity of bubble-point liquid.

In the case of 1-butene, the necessary volumetric data including the rates of change of bubble-point and dew-point specific volumes with temperature and the rate of change of vapor pressure with temperature were obtained from published data (3). It is believed that these values for 1-butene were known with sufficient accuracy to avoid introducing an uncertainty greater than 0.2 per cent in the final results. Since no volumetric data for 1-pentene were available for the temperature range covered by this investigation it was necessary to utilize information based upon n-pentane (4) and the law of corresponding states (5) to establish the requisite volumetric behavior. (This procedure should give results of sufficient accuracy for this use.) The

evaluation of the related terms of equation (3) by such methods did not introduce added uncertainties of more than 0.3 per cent in the final value of the isobaric heat capacity of the bubble-point liquid. Values of the isobaric heat capacity at dew point for 1-butene and 1-pentene were taken as equal to the equivalent values for n-butane (6) and n-pentane (6). It is believed that the application of these data to the corresponding olefinic hydrocarbons did not introduce a significant uncertainty in the results obtained from equation (3).

Apparatus and Procedure

The calorimetric equipment used in these studies was substantially the same as that employed in earlier investigations (7,8). In principle, the equipment consisted of a cylindrical steel container with hemispherical closures within which the hydrocarbon liquid was confined. Thermal equilibrium within the container was obtained by means of a small impeller rotating around an axis coincident with that of the calorimeter. Energy was added electrically to the interior of the calorimeter by means of a short length of glass-insulated constantan wire encased within a stainless steel tube approximately 0.05 inch in diameter. The ends of the steel tube were brought through the wall of the calorimeter with a sealed joint. The quantity of electrical energy added to the calorimeter was determined by conventional volt box and standard resistance techniques. A potentiometer was employed to measure the electromotive force applied and the current flowing through

the calorimeter heater. It is believed that the rate of electrical energy addition to the calorimeter was known with an uncertainty of less than 0.05 per cent. Electrical energy was added to the calorimeter for approximately 500 seconds in the case of each measurement. The uncertainty in the determination of the total energy thus added to the equipment was less than 0.1 per cent. The timing of the other events associated with the measurement of heat capacity was sufficiently accurate as to introduce only a negligible uncertainty in the result.

In order to decrease the thermal losses, the calorimeter was surrounded by an adiabatic jacket and the space between the jacket and the calorimeter was evacuated. Provision was made for the automatic maintenance of the average temperature of the interior surface of the jacket at substantially that of the exterior surface of the calorimeter. Measurements were carried out to establish the magnitude of the thermal losses as a function of the measured temperature difference between the calorimeter and the wall of the jacket. The energy transfers between the calorimeter and the jacket were in almost all cases less than 1 per cent of the energy added to the unit. The magnitude of this transfer was established with reasonable accuracy and it is believed that the uncertainties resulting from thermal losses were not greater than 0.15 per cent of the corrected values of the energy added to the calorimeter.

The scheme of measurement involved the addition of a known weight of 1-butene or 1-pentene to the calorimeter and determination

of the net energy required to raise the temperature of the calorimeter and contents through a known temperature interval. For the purposes of these calculations it was assumed for the particular temperature interval in question that the following equation was applicable:

$$\frac{g}{dT} = \frac{Q}{T_B - T_A} \qquad (4)$$

The left-hand side of equation (4) was considered to apply at the mean of the initial and final temperatures. After completion of one such series of measurements which extended over the entire temperature range investigated, additional material was introduced into the calorimeter and the sequence of measurements repeated. For the most part the quantity of energy added electrically was adjusted to yield an over-all temperature rise of approximately 6°F. An effort was made to carry out each set of determinations in accordance with a standardized procedure. The period allowed for the attainment of equilibrium after the addition of energy was used as the conditioning period for the next step. Figure 1 shows a typical set of time-temperature measurements for the calorimeter when it contains 0.1987 pound of 1-butene. In this instance, thermal equilibrium was closely attained within 8 minutes after termination of the addition of energy. The variation in temperature in the calorimeter with time beyond this period was less than 0.002°F per minute. Similar variations in temperature with time were obtained in the studies of 1-pentene.

The samples were introduced into the calorimeter by use of high vacuum and weighing bomb techniques (9). It is believed that the weight of the sample introduced into the calorimeter was known within 0.02 per cent. In order to check upon this quantity and to ascertain that no loss occurred, the samples were withdrawn after the completion of each set of measurements. It was found in all cases that agreement between the weight of material added and that withdrawn was within 0.1 per cent.

Materials

The 1-butene used in this investigation was prepared by the dehydration of normal butyl alcohol with an aluminum oxide catalyst at a temperature of 660°F. The crude material was fractionated twice at atmospheric pressure in a column packed with glass rings at a reflux ratio of 5 to 1. Approximately 15 per cent of the overhead was discarded at the beginning and end of each fractionation. The purified 1-butene exhibited a range in boiling point at atmospheric pressure of less than 0.2°F.

The 1-pentene was of research grade and was purchased from the Phillips Petroleum Company. The manufacturer's analyses indicated that it contained less than 0.6 mole per cent of hydrocarbon other than 1-pentene, the probable impurity being isopentane. Because of the relatively small quantity of the sample available, the material was utilized without further purification except for two partial condensations at liquid air temperature to remove any significant quantities of dissolved noncondensable gases. The 1-pentene after purification was

handled in the same way as the 1-butene and was introduced into the calorimeter by weighing bomb techniques (9).

Experimental Measurements

The experimental values obtained for the heat capacity of the bomb containing two different quantities of 1-butene are presented in Figure 2. The average deviation of the experimental points presented is 1.2 per cent of the difference between the two curves. As a part of Table I are recorded experimental values of the heat capacity of the calorimeter and its contents at several temperatures. This intermediate information is presented in order that the results may be re-evaluated if at a later date more accurate and complete volumetric measurements are available. The weights of the samples are included in Table I.

In Figure 3 is presented information about the heat capacity of the calorimeter and its contents for three different quantities of 1-pentene. The average deviation of the experimental points shown from the curves drawn for this substance is also 1.2 per cent of the difference between the curves. Table I contains values at several temperatures of the heat capacity of the calorimeter with the three samples of 1-pentene.

Results

Values of the isobaric heat capacity at bubble point for 1-butene and 1-pentene are recorded in Table II. A consideration of

the accuracy of the measurement of the individual quantities involved indicates an uncertainty of approximately 1 per cent in the tabulated values. In order to permit a direct comparison of the isobaric heat capacities recorded in Table II with the earlier measurements of Aston (1) and Huffman (2), a graphical representation of the data has been given in Figure 4. Reasonable agreement with the earlier measurements was obtained in the case of both compounds. The curve shown for 1-butene represents the best estimate of the authors for the combined experimental results of Aston (1) and the new measurements presented in this discussion. The present data indicate a slightly smaller increase in the isobaric heat capacity at bubble point with temperature for 1-pentene than would have been predicted from the earlier measurements of Huffman and co-workers (2) and the two sets of data have been indicated by separate curves. However, the discrepancy appears to be less than the combined uncertainty of the two sets of data.

Acknowledgment

Financial assistance from the California Research Corporation and the interest of H. G. Vesper of that organization have made this work possible. The equipment employed was developed as a part of the activities of Project 37 of the American Petroleum Institute. The cooperation of the American Petroleum Institute in permitting the use of the calorimeter equipment in this investigation is acknowledged.

Nomenclature

C_p isobaric heat capacity, (B.t.u./lb)/°F

$\underline{E}$ total internal energy, B.t.u.

E specific internal energy, B.t.u./lb

ℓ_p latent heat of pressure change, (B.t.u./lb)/(lb/sq.in.)

m weight of material in calorimeter, lb

P pressure, lb/sq.in. abs

$\underline{Q}$ heat associated with process, B.t.u.

$\underline{q}$ heat associated with infinitesimal change in state, B.t.u.

T thermodynamic temperature, °Rankine

V specific volume, cu.ft/lb

Subscripts

A,B state A and state B

b bubble point

d dew point

1,2 conditions with different quantities of sample in calorimeter

Superscript

" two-phase state

References

(1) Aston, J. G., Fink, H. L., Bestful, A., Pace, E. L., and Szasz, G. J., J. Am. Chem. Soc., 68, 52 (1946).

(2) Todd, S. S., Oliver, G. D., and Huffman, H. M., J. Am. Chem. Soc., 69, 1519 (1947).

(3) Olds, R. H., Sage, B. H., and Lacey, W. N., Ind. Eng. Chem., 38, 301 (1946).

(4) Sage, B. H. and Lacey, W. N., Ind. Eng. Chem., 34, 730 (1942).

(5) Gibbs, J. W., Trans. Conn. Acad., 3, 108 (1876).

(6) Kennedy, E. R., Sage, B. H., and Lacey, W. N., Ind. Eng. Chem., 28, 718 (1936).

(7) Sage, B. H., Evans, H. D., and Lacey, W. N., Ind. Eng. Chem., 31, 763 (1939).

(8) Budenholzer, R. A., Sage, B. H., and Lacey, W. N., Ind. Eng. Chem., 35, 1214 (1943).

(9) Sage, B. H., and Lacey, W. N., Trans. Am. Inst. Mining Met. Engrs., 136, 136 (1940).

Table I. Heat Capacity of Calorimeter and Contents

1-Butene

0.19872 lb[a]		0.052025 lb	
Temp. °F	q/dT B.t.u./°F	Temp. °F	q/dT B.t.u./°F
116.10	0.40646	101.93	0.32119
121.62	0.40744	115.47	0.33067
127.23	0.40962	122.27	0.33159
132.60	0.41223	128.96	0.33494
137.80	0.41825	135.65	0.33645
143.20	0.42020	142.22	0.33904
148.81	0.41764	148.73	0.34098
154.24	0.42274	155.25	0.34264
159.56	0.42609	161.73	0.34891
164.71	0.42789	181.29	0.35661
175.59	0.43529	187.65	0.35520

[a] Weight of material in calorimeter

Table I. (cont'd)

1-Pentene

0.14215 lb		0.14200 lb		0.03700 lb	
Temp. °F	q/dT B.t.u./°F	Temp. °F	q/dT B.t.u./°F	Temp. °F	q/dT B.t.u./°F
104.43	0.36221	113.83	0.36413	91.40	0.30121
110.82	0.36562	120.57	0.36732	99.84	0.30402
117.26	0.36702	127.00	0.36975	107.83	0.30966
123.50	0.36792	133.85	0.37206	115.51	0.31142
129.84	0.37039	140.57	0.37254	123.19	0.31295
142.46	0.37327	147.21	0.37660	130.92	0.31517
148.71	0.37814	153.70	0.37913	138.66	0.31831
154.93	0.38081	160.26	0.38162	147.27	0.31942
161.05	0.37894	166.71	0.38249	154.76	0.32272
167.18	0.38423	173.35	0.38428	162.02	0.32536
173.34	0.38560	179.74	0.38675	169.25	0.32748
182.60	0.38621	186.18	0.38974	191.32	0.33337
191.52	0.38982	192.49	0.39139	198.45	0.33765
197.71	0.39246	198.76	0.39423		
204.20	0.39362	204.97	0.39578		

Table II. Isobaric Heat Capacities of 1-Butene and 1-Pentene at Bubble Point

Temp. °F	1-Butene (B.t.u./lb)/°F	1-Pentene (B.t.u./lb)/°F
70[a]	0.548	0.526
80[a]	0.555	0.530
90[a]	0.562	0.535
100	0.5682	0.5391
110	0.5752	0.5431
120	0.5827	0.5474
130	0.5910	0.5518
140	0.6005	0.5560
150	0.6105	0.5600
160	0.6232	0.5641
170	0.6380	0.5683
180	0.6570	0.5727
190	0.6812	0.5774
200	0.7112	0.5827
210[a]	0.746	0.589
220[a]	0.785	0.595

[a] Extrapolated

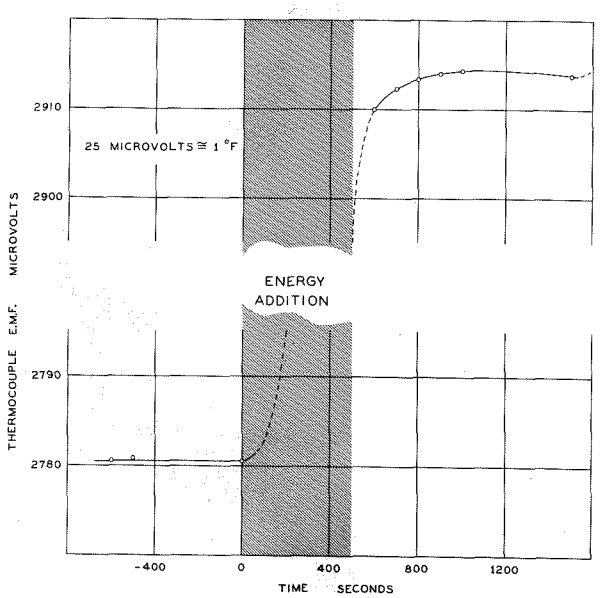

Figure 1. Variation in Temperature of Calorimeter with Time

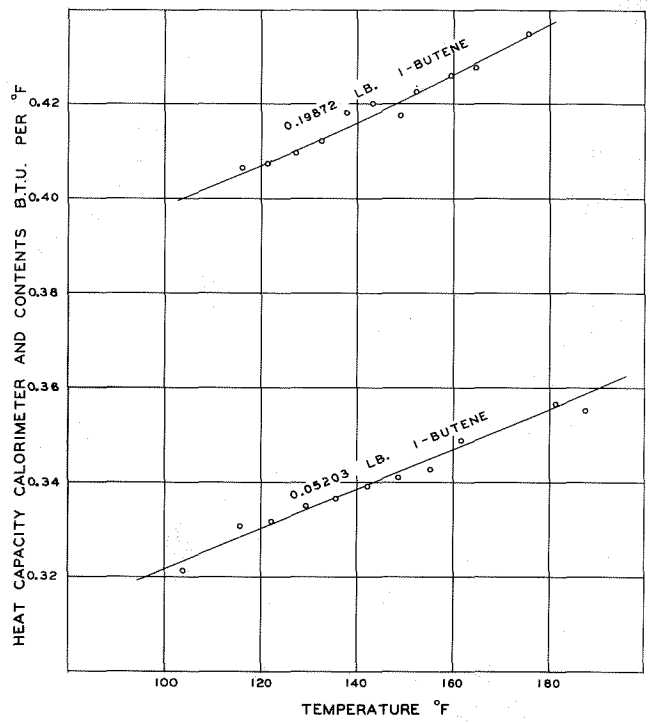

Figure 2. Calorimetric Measurements for 1-Butene

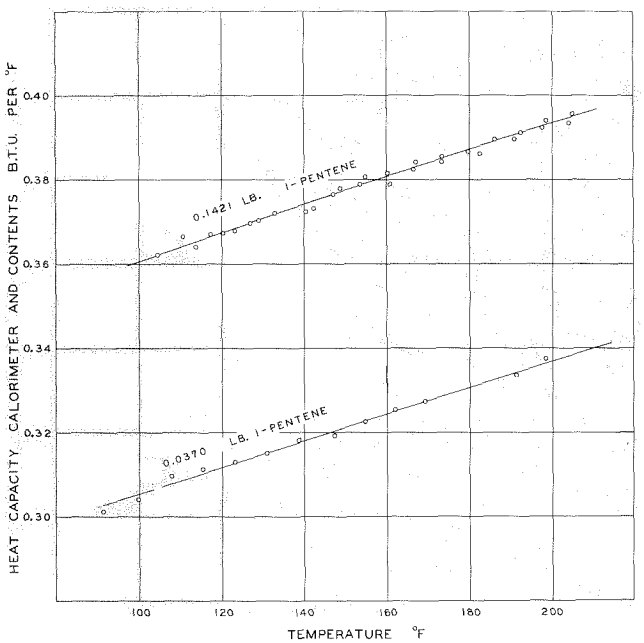

Figure 3. Calorimetric Measurements for 1-Pentene

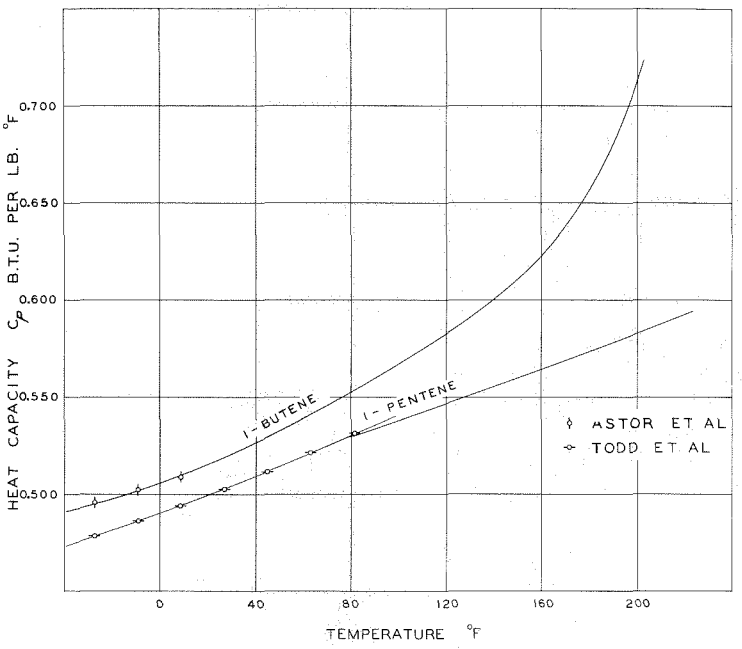

Figure 4. Isobaric Heat Capacities of 1-Butene and 1-Pentene at Bubble Point

Part III

Mass Transfer in a Turbulent Air Stream

Introduction

The development of methods of predicting the behavior of operations such as humidification, drying, and diffusion is dependent upon advancement in the science of fluid mechanics. In these operations a concentration gradient of a component results in the transfer of this material by a process of molecular or turbulent diffusion. The mechanism of molecular diffusion based upon the kinetic theory appears to describe experimentally established behavior satisfactorily. In turbulent diffusion the finite motion of masses of fluid termed eddies plays a major part in the diffusional process. These eddies are formed as a result of turbulence defined by Taylor and von Karman (1) as "an irregular motion which in general makes its appearance in fluids, gaseous or liquid, when they flow past solid surfaces or even when neighboring streams of the same fluid flow past or over one another." Turbulence is usually described by its intensity and scale. The intensity of turbulence is the magnitude of the time average of the root mean square of the vectors of the deviating velocity at a given point within the stream. The deviating vector velocities are the three mutually perpendicular components of the transient velocity superimposed upon the gross time average velocity of the stream at the point in question. The scale factor may be considered as the average size of the individual eddies. The analogous quantities in molecular diffusion are temperature and mean free path for the intensity and scale, respectively. Techniques have been devised for

establishing these two measures of turbulence by the use of hot wire anemometers and appropriate electronic instrumentation. A summary of these methods has been presented by Dryden (2).

Eddies transfer finite quantities of material from one point to another as a result of their random motion. This process under many conditions of industrial interest transfers material at many times the rate which would result from molecular diffusion. Since molecular and turbulent diffusion are somewhat similar, equations analogous to those used in molecular diffusion may be considered as being applicable to turbulent diffusion. Considering both types of diffusion the total rate of material transfer may be written as

$$N = -(\epsilon_d + D)\frac{dC}{dx} \tag{1}$$

Since the magnitude of the molecular diffusivity D is usually much smaller than the eddy diffusivity, ϵ_d equation (1), when applied to fully developed turbulent flow, is often written (6)

$$N = -\epsilon_d \frac{dC}{dx} \tag{2}$$

Taylor (3) has shown this equation to apply only in cases where the diffusion distance is large compared with the Taylor mixing length which is defined by

$$\ell_x = \int_0^\infty R_x \, dx \tag{3}$$

This equation relates the mixing length or scale factor ℓ_x to the term R_x a correlation factor between the deviating velocities. Another quantity which is useful in dealing with turbulent flow is the eddy viscosity which is analogous to the kinematic viscosity. These terms are related to the shear in the following way:

$$\tau = \rho(\epsilon_v + \nu)\frac{du}{dx} \tag{4}$$

In the foregoing relation as in equation (2) the molecular or kinematic viscosity ν may be neglected and equation (4) may be rewritten as

$$\tau = \rho\epsilon_v\frac{du}{dx} \tag{5}$$

The proportionality factor ϵ_v, called the eddy viscosity, is related to the transfer of momentum in a turbulent stream. Various investigators have advanced theories pertaining to the relation between the transfer of momentum and the transfer of material. The results indicate that the two factors ϵ_d and ϵ_v should be proportional. However, Dryden (2) and Liepmann (4) have indicated that the proportional relation between the eddy viscosity and eddy diffusivity should exist only under certain specific conditions of flow.

Sherwood and Woertz (5) reported some corresponding values of the eddy viscosity and eddy diffusivity for the case of two-dimensional turbulent flow between parallel plates. Their experimental measurements

indicated the following empirical relationship in which α was found to be 1.6 under the conditions of their investigation:

$$\epsilon_d = \alpha \epsilon_v \tag{6}$$

Towle and Sherwood (6) have reported data on the diffusion of hydrogen and carbon dioxide from a point source in a turbulent air stream, and Kalinske and Pien (7) determined eddy diffusivities for the mixing of material from a point source in a turbulent stream of water. Results indicate that the eddy diffusivity is nearly constant in the turbulent core of the stream and that the product of the specific weight and the eddy diffusivity is related to the Reynolds number of the flowing stream. As a part of a study of combustion in the gas phase an experimental study was made of the macroscopic diffusion under turbulent flow conditions of natural gas into air.

Equipment

The equipment employed in this study provided a horizontal annular air stream of circular section into which a coaxial stream of natural gas was admitted. Provisions were made to determine the velocity and composition of the mixed stream at nine stations downstream from the point of initial mixing.

A schematic diagram of the arrangement of the apparatus is presented in Figure 1. A centrifugal blower A drew air through a heat interchanger B which was used to obtain rough temperature regulation of the incoming air stream. After the blower A the air passed

through the electric heaters C which supplied energy for the final temperature adjustment. The rate of fluid flow was measured by means of the venturi meter D. The pressure differential at the venturi meter was determined with an air-kerosene manometer used in conjunction with a vertical component cathetometer. After passing through appropriate ducts E,F,G and past a mercury-in-glass thermal regulator H, the air entered the working section J. This section was constructed of a copper tube with an inside diameter of 4 inches. This inner tube was surrounded by an air jacket 6 inches in diameter.

Natural gas was admitted coaxially with the air stream through a copper tube 1 inch in diameter which is shown in Figure 2. The exterior walls of this tube were tapered at an angle of 0.6 degree in order to obtain a wall thickness of less than 0.005 inch at the point of mixing. This tapered wall tube was used in order to decrease the disturbances resulting from an abrupt change in section of the conduit. The temperature of the natural gas was controlled by electric heaters which were located on the exterior of a section of the conduit K and located upstream of the calibrated orifice meter L. This orifice meter was used to determine the rate of flow of the natural gas. The differential pressure at the orifice meter was determined by means of a kerosene-in-glass manometer used in conjunction with a cathetometer. The flow rate of the natural gas was controlled to within 0.5 per cent of a predetermined value by a manually operated throttle valve in the supply line. Equipment for

the control of temperature permitted both the air and natural gas to be maintained within 0.1°F of a predetermined value. The rate of flow of air was controlled to within 0.5 per cent of the desired value by means of varying the speed of the motor driving the centrifugal blower A in Figure 1. After the mixing stream passed through the working section J, the mixture was ignited outside of the building at the burner M.

The arrangement of the working section is shown in Figure 3. Nine sampling ports were located at distances varying from 3 to 100 inches downstream from the point of initial mixing and their location is shown in Figure 3. The sampling ports were provided with removable plugs which were flush with the interior surface of the copper working section. Each of these plugs could be removed and replaced by a pitot tube assembly. The pitot tube was arranged so as to permit the impact pressure to be determined as a function of radius at each station. The dynamic pressure was measured with a kerosene-in-glass manometer used in conjunction with a vertical component cathetometer or by means of a micromanometer of the design that is shown in Figure 4. The latter instrument was used when the pressure differential was less than 2.5 inches of kerosene. The pitot tube was also employed to withdraw samples from the working section to permit the composition of the fluid at that point to be determined. The composition of the air-natural gas mixture was established from measurements of the specific weight of a sample of the mixture. The specific weight measurements were accomplished by weighing bulb techniques. The gas samples were

withdrawn at a rate such that the velocity of the gas entering the pitot tube was equal to that of the flow stream. The glass weighing bulbs used in the specific weight measurements were immersed in an agitated air bath during filling. The temperature of the air was controlled within 0.1°F at 100°F. The pressure in the weighing bulbs was measured relative to that of the atmosphere by a kerosene-in-glass manometer. When cooled to room temperature the bulbs were weighed on an analytical balance with a relative uncertainty of 0.2 milligram. Since the weights of the gas samples in the bulbs varied from 400 to 600 milligrams over the range of composition of interest in this investigation, the specific weight of the samples was determined with an uncertainty of approximately 0.3 per cent. The correction for the deviation of the natural gas-air mixtures from ideal solutions (8) was not significant in establishing the composition from the specific weight determinations. In addition the influence of humidity of the air upon the specific weight of the mixtures was taken into account.

Procedure and Results

The composition and the flow patterns were studied at the following gross velocities: 25, 50, and 100 feet per second. The annular air stream and natural gas stream were arbitrarily held at the same gross velocity and temperature. The velocity at each of the nine stations was determined at intervals of 0.1 inch across the

working section. Specific weight determinations were made upon samples taken at the same positions when the sample contained more than 1 mole per cent natural gas. Knowledge of the specific weight of the natural gas and air permitted the calculation of the composition of natural gas-air mixtures at the point where a sample was withdrawn. Representative velocity and composition profiles are presented in Figures 5 through 7.

Eddy Diffusivity and Eddy Viscosity

The combination of equation (2) with a material balance for one of the components in the mixing region of the flowing stream results in the following equation:

$$\frac{\partial}{\partial z}(r C_g u_z) + \frac{\partial}{\partial r}(r C_g u_r) + \frac{\partial}{\partial \theta}(C_g u_\theta) =$$

$$\frac{\partial}{\partial z}(r \epsilon_{d_z} \frac{\partial C_g}{\partial z}) + \frac{\partial}{\partial r}(r \epsilon_{d_r} \frac{\partial C_g}{\partial r}) + \frac{\partial}{r \partial \theta}(\epsilon_{d_\theta} \frac{\partial C_g}{\partial \theta}) \qquad (7)$$

Another useful equation may be obtained if it is assumed that the partial molal volume of each component is equal to the molal volume of the mixture. Then the volume of material entering any element may be equated to that leaving the element in the same period. This assumption leads to the following expression:

$$\frac{\partial}{\partial z}(u_z r) + \frac{\partial}{\partial r}(u_r r) + \frac{\partial}{\partial \theta}(u_\theta) = 0 \qquad (8)$$

If the diffusion in the axial direction is neglected and it is assumed that the composition and velocity patterns are symmetrical about the axis of flow, equations (7) and (8) may be combined to yield

$$\epsilon_{d_r} = \frac{\frac{\partial}{\partial z}\int_0^r C_g u_z r\,dr - C_g \frac{\partial}{\partial z}\int_0^r r u_z\,dr}{r\,\frac{\partial C_g}{\partial r}} \qquad (9)$$

The representative composition traverse shown in Figure 7 which was obtained at gross air and gas velocities of 25 feet per second indicates the pronounced effect of gravity on the stream. The natural gas tends to rise in the central portion of the working section while the air tends to accumulate on the lower part of the copper tube. Therefore at low velocities it is not valid to assume that the composition pattern is symmetrical about the axis of flow, and a more complex analysis must be made for conditions typified by the arrangement of the working section.

Equations (7) and (8) may be combined to give the following relatively simple expression:

$$\epsilon_{d_r} = \frac{\int_0^r u_z r \frac{\partial C_g}{\partial z}\,dr + \int_0^r u_r r \frac{\partial C_g}{\partial r}\,dr}{r\,\frac{\partial C_g}{\partial r}} \qquad (10)$$

if it is assumed that $\frac{\partial^2 C_g}{\partial z^2} = \frac{\partial^2 C_g}{\partial \theta^2} = 0$ and that the product of $\frac{\partial \epsilon_{d_r}}{\partial z}$ and $\frac{\partial C_g}{\partial z}$ is small compared to the other terms.

The coordinate system at each station may then be moved to the point corresponding to a maximum in the molal fraction of the natural gas without introducing any significant added uncertainty. The assumptions employed in the derivation of equation (10) appear most valid when the coordinates are thus transformed.

The solution of equation (10) involves a knowledge of the magnitude of the radial component of velocity. In the vertical plane the value of u_r was estimated by computing the rate of rise of the point of maximum natural gas concentration at each station.

An approximate integration of equation (7) may be obtained by application of suitable assumptions. If a velocity and composition pattern which is symmetrical about the axis of the working section is considered, equation (7) reduces to

$$r\frac{\partial}{\partial y}(C_g u_y) + \frac{\partial}{\partial r}(C_g u_r r) = r\frac{\partial}{\partial y}\left(\epsilon_{d_y}\frac{\partial C_g}{\partial y}\right) + \frac{\partial}{\partial r}\left(r\epsilon_{d_r}\frac{\partial C_g}{\partial r}\right) \quad (11)$$

Neglecting the axial diffusion, the variation of ϵ_{d_r} with radius and the variation of u_y with y equation (11) reduces to

$$\frac{\partial^2 C_g}{\partial r^2} + \frac{1}{r}\frac{\partial C_g}{\partial r} = \frac{u_y}{\epsilon_{d_r}}\frac{\partial C_g}{\partial y} \quad (12)$$

If $\frac{u_y}{\epsilon_{d_r}}$ is treated as constant, the general solution of this partial differential equation may be expressed as

$$C_g = e^{-\frac{\beta^2 \epsilon_{d_r} y}{u_y}}\left[\gamma J_0(\beta r) + \delta K_0(\beta r)\right] \quad (13)$$

The boundary conditions obtaining in the working section may be described as

$$r = a \qquad \frac{\partial C_g}{\partial r} = 0$$

$$z = 0 \quad C_g = f(r) \qquad 0 \leq r \leq b \quad f(r) = 1 = n_g \qquad b \leq r \leq a \quad f(r) = 0 \tag{14}$$

where n_g is a reduced value of C_g and at constant temperature is identical to the mole fraction. These conditions applied to equation (13) result in the following infinite series:

$$n_g = \frac{2}{a^2} \sum_{i=1}^{i=\infty} \frac{e^{-\frac{\beta_i^2 \epsilon_{d_r} z}{u_z}} b J_1(\beta_i b) J_0(\beta_i r)}{\beta_i \left[J_0(\beta_i a)\right]^2} \tag{15}$$

where β_i represents roots of the following equation:

$$J_1(\beta a) = 0 \tag{16}$$

The solution to equation (15) that is obtained by taking a = 1.91 inches and b = 0.47 inch is shown by the solid lines in Figure 8. In this figure n_g is plotted as a function of $\frac{\epsilon_{d_r} z}{u_z}$.

It is possible to derive an expression relating the eddy viscosity to the measurable quantities. By consideration of an axial force

balance on a small element in the flowing stream the following relationship is obtained:

$$\frac{\partial}{\partial r}(r\rho u_y u_r) + \frac{\partial}{\partial y}(r\rho u_y^2) + g\frac{\partial P}{\partial y} r = \frac{\partial(r\tau_{r,y})}{\partial r} + \frac{\partial \tau_{\theta,y}}{\partial \theta} \qquad (17)$$

Equation (17) may be simplified if it is assumed that $\frac{\partial P}{\partial y}$ is independent of the radius and that the flow pattern is symmetrical about the axis of the duct. Using these assumptions, substituting the value of eddy viscosity as defined by equation (5), and eliminating u_r by equation (8) the following expression results:

$$\epsilon_{v_r} = \frac{\frac{\partial}{\partial y}\int_0^r \rho u_y^2 dr^2 - \rho u_y \frac{\partial}{\partial y}\int_0^r u_y dr^2 + r^2 g \frac{\partial \rho}{\partial y}}{2r \frac{\partial u_y}{\partial r}} \qquad (18)$$

Treatment of Data

The measurements made at gross air and gas velocity of 100 feet per second were employed in conjunction with the graphical solutions of equation (9) to obtain the values of ϵ_{d_r} that are presented in Table I. The apparent variation of the eddy diffusivity with radial

distance from the axis of the flow channel is depicted in Figure 9. In this figure the various straight lines representing different distances downstream from the point of gas injection were determined by application of the method of least squares to the information recorded in Table I. The average standard deviation of the experimental points from the lines in Figure 9 is 0.17 square inch per second.

In Figure 8 the experimental values of the mole fraction which were determined at a gross velocity of 100 feet per second are superimposed upon the solution of equation (15). The best agreement was obtained by taking $\frac{\epsilon d_r}{u_z}$ equal to 1.86×10^{-3} inches. This corresponds to an average value of ϵd_r in the mixing region of approximately 2.3 square inches per second. This figure compares favorably with the average value of 2.5 square inches per second obtained from Figure 9. It may be predicted from Figure 8 that in certain regions significant variations from the average eddy diffusivity will exist. Thus the deviation of experimental compositions at small values of r and y indicate that the actual value of in the region is higher than average. This prediction is confirmed by the data presented in Figure 9.

At gross air and gas velocities of 25 and 50 feet per second the influence of gravity upon the flowing stream was sufficiently pronounced that the assumptions employed in deriving equation (9) were no longer valid. Using the experimental data obtained at these two velocities equation (10) was solved graphically to yield the eddy diffusivities presented in Table I. Each of the diffusivities

recorded in this table was the average of the two values determined at an equal distance on either side of the axis of flow. The figures in Table I were treated by the method of least squares and the resulting straight lines corresponding to different axial distances are depicted in Figures 10 and 11. The average standard deviation in the eddy diffusivities at gross velocities of 25 and 50 feet per second is 0.09 and 0.17 square inch per second, respectively.

The studies made at each of the three velocities show several trends. The eddy diffusivity appears to decrease markedly with increasing radial distance near the region where the natural gas is injected and approaches a nearly constant value at a section 10 to 15 diameters downstream. In addition the magnitude of the eddy diffusivity at a particular point in the turbulent stream is roughly proportional to the Reynolds number. There is a decrease in the value of the eddy diffusivity with increasing distance from the point of initial mixing. The minimum diffusivity occurs at a section from 10 to 25 diameters downstream from the point of mixing.

An attempt was made to estimate the value of the eddy viscosity by a graphical solution of equation (18). However, the combined uncertainty of the several terms in equation (18) rendered the computation invalid.

The uncertainty of the computed values of the eddy diffusivity is to a large extent the result of the method used in the graphical determinations of the derivatives of the relationships involving large curvatures.

Discussion

The relation between Reynolds number, eddy diffusivity, and specific weight reported in studies of Sherwood, Woertz, and Towle (5,6) provides a means of estimating the magnitude of the eddy diffusivity in certain regions of the flowing stream in the present work. Since the Reynolds number of the stream of natural gas in the injection conduit may be established, the magnitude of the eddy diffusivity in regions immediately adjacent to the exit of this pipe might be expected to correspond with the values predicted from this Reynolds number. Confirmation of this viewpoint was found from the present studies, however the average values of eddy diffusivity obtained from Figures 9, 10, and 11 are approximately 20 per cent higher than those predicted. In a like manner it might be possible to predict the eddy diffusivity at such a distance downstream from the point of initial mixing that normal turbulent flow has been restored. Comparison of the present experimental data with that of Sherwood, Woertz, and Towle (5,6) indicates predicted values of the eddy diffusivity which are 2.5 times those experimentally determined at a distance of 95.25 inches from the point of natural gas injection.

Acknowledgment

This experimental work was made possible by the financial support of the United States Army Air Force through the Jet Propulsion Laboratory, Pasadena, California. The assistance of

Mr. Theodore Wadsley and Mr. Forrest Gilmore in the accumulation of the experimental data and the aid of Mr. Robert Sears in the preparation of this report are gratefully acknowledged.

Nomenclature

a	radius of natural gas pipe line, 1.91 in.
b	radius of working section, 0.47 in.
C	concentration, lb.mole/cu.in.
D	molecular diffusion constant, sq.in./sec
e	base of natural logarithms
g	acceleration due to gravity, ft/sq.sec
J	Bessel function of the first kind
K	Bessel function of the second kind
l	mixing length, in.
N	molal rate of diffusion per unit area, (mole/sec)/sq.in.
n	mole fraction
R	correlation factor between deviating velocities
r	radial distance from axis of working section, in.
u	velocity, in./sec
x	length, in.
y	axial distance in working section from point of initial mixing, in.

α constant of proportionality between ϵ_d and ϵ_ν

β a constant

β_i roots of the equation $J_1(\beta a) = 0$

γ a constant

δ a constant

ϵ_d eddy diffusivity, sq.in./sec

ϵ_ν eddy viscosity, sq.in./sec

ν kinematic viscosity, sq.in./sec

ρ specific weight, lb/cu.in.

θ angular displacement about axis of working section

τ shear stress per unit area parallel to flow, lb/in./sq.sec

Subscripts

g refers to natural gas

r refers to radial direction

y refers to axial direction

θ refers to angular direction

0 refers to Bessel Function of zero order

1 refers to Bessel Function of first order

References

(1) von Karman, Th., Roy. Aero. Soc., 41, 1109 (1937).

(2) Dryden, H. L., Ind. Eng. Chem., 31, 416 (1939).

(3) Taylor, G. I., Proc. Roy. Soc., 151A, 421 (1935).

(4) Liepmann, H. W. and Laufer, J., Nat. Ad. Comm. Aero., Tech. Pub. No. 1257 (1947).

(5) Sherwood, T. K. and Woertz, B. B., Trans. Am. Inst. Chem. Eng., 35, 517 (1939).

(6) Towle, W. L. and Sherwood, T. K., Ind. Eng. Chem., 31, 457 (1939).

(7) Kalinske, A. A. and Pien, C. L., Ind. Eng. Chem., 36, 220 (1944).

(8) Lewis, G. N., Proc. Am. Acad. Arts Sci., 43, 259 (1907).

Table I. Average Eddy Diffusivity*

Radial Distance from Axis of Duct, in.	Distance Downstream from Point of Initial Mixing, in. 7.25	11.25	17.25	23.25	35.25	47.25	71.25	95.25
			Gross Velocity 25 ft/sec					
0	---	---	0.0098	---	0.0049	0.0031	0.0047	0.0103
0.1	---	0.0104	---	0.0077	0.0037	0.0029	0.0049	0.0093
0.2	0.0127	0.0094	0.0076	0.0067	0.0033	0.0027	0.0052	0.0095
0.3	0.0069	0.0082	0.0074	0.0072	0.0036	0.0030	0.0063	0.0089
0.4	0.0067	0.0069	0.0075	0.0073	0.0057	---	---	0.0095
0.5	0.0057	0.0063	0.0067	0.0067	0.0058	---	---	---
0.6	0.0058	0.0053	0.0062	0.0069	0.0057	---	---	---
0.7	0.0047	0.0047	0.0060	0.0076	0.0062	---	---	---
0.8	---	0.0034	0.0057	0.0076	0.0067	---	---	---
0.9	---	0.0034	---	---	---	---	---	---

* Average eddy diffusivity is expressed in sq.ft/sec

Table I. (Cont'd)

Radial Distance from Axis of Duct, in.	Distance Downstream from Point of Initial Mixing, in. 7.25	11.25	17.25	23.25	35.25	47.25	71.25	95.25
			Gross Velocity 50 ft/sec					
0.1	0.0175	0.0145	0.0135	0.0106	0.0062	0.0051	0.0040	0.0054
0.2	0.0160	0.0155	0.0145	0.0104	0.0078	0.0060	0.0047	0.0057
0.3	0.0117	0.0160	0.0150	0.0110	0.0092	0.0066	0.0045	0.0061
0.4	0.0125	0.0160	0.0130	0.0125	0.0104	0.0064	0.0046	0.0050
0.5	0.0130	0.0100	0.0109	0.0115	0.0100	0.0069	0.0045	0.0096
0.6	---	---	0.0105	0.0100	0.0097	0.0081	0.0047	0.0092
0.7	---	---	0.0112	0.0101	0.0115	0.0080	0.0052	0.0098
0.8	---	---	0.0120	0.0101	0.0115	0.0101	0.0054	0.0102

Table I. (Cont'd)

Radial Distance from Axis of Duct, in.	Distance Downstream from Point of Initial Mixing, in. 7.25	11.25	17.25	23.25	35.25	47.25	71.25	95.25
	Gross Velocity 100 ft/sec							
0.1	---	---	0.0281	---	---	---	0.0146	---
0.2	0.0311	0.0247	0.0223	0.0262	0.0212	0.0154	0.0133	---
0.3	0.0278	0.0231	0.0218	0.0240	0.0224	0.0174	0.0128	0.0114
0.4	0.0187	0.0198	0.0210	0.0234	0.0222	0.0174	0.0106	0.0090
0.5	0.0172	0.0200	0.0198	0.0197	0.0201	0.0164	0.0096	0.0106
0.6	0.0210	0.0228	0.0186	0.0192	0.0182	0.0154	0.0088	0.0116
0.7	0.0155	0.0140	0.0156	0.0176	0.0174	0.0150	0.0102	0.0110
0.8	0.0171	0.0156	0.0142	0.0157	0.0164	0.0149	0.0129	---
0.9	0.0168	---	---	0.0163	---	---	0.0143	0.0111
1.0	---	---	---	0.0152	---	---	---	0.0125
1.1	---	---	---	---	---	---	---	0.0134

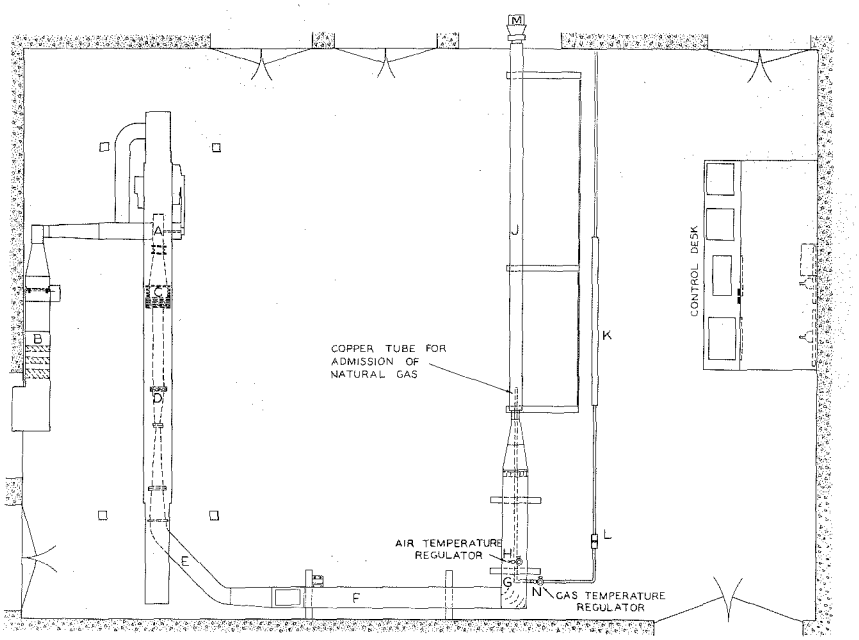

Figure 1. Schematic Arrangement of the Equipment

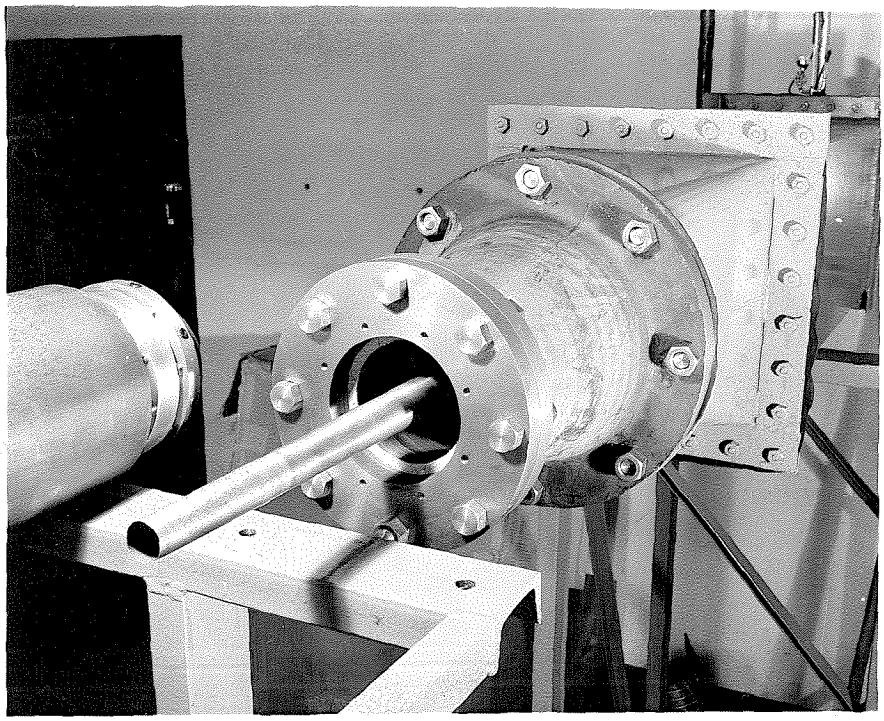

Figure 2. The Exterior of the Natural Gas Injection Tube

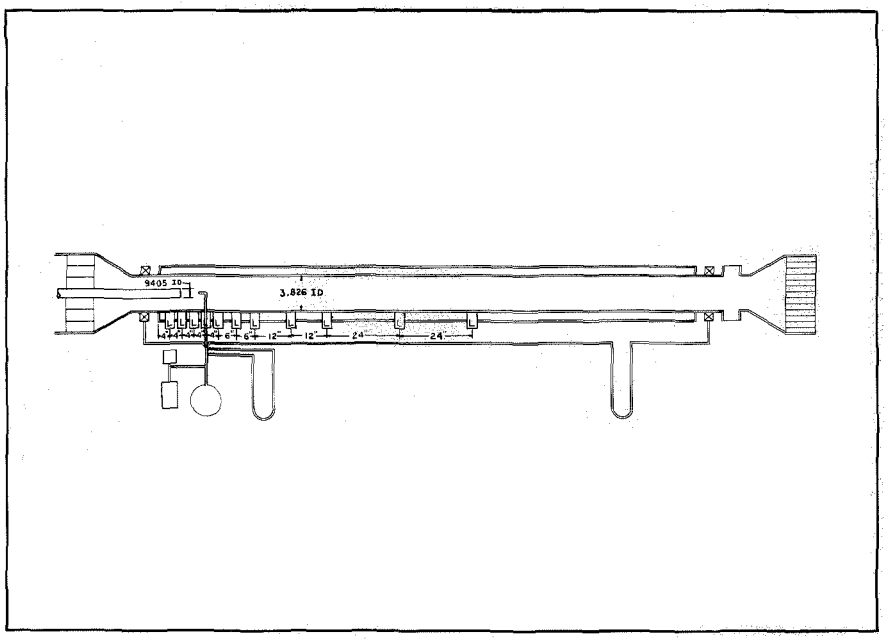

Figure 3. Schematic Arrangement of the Working Section

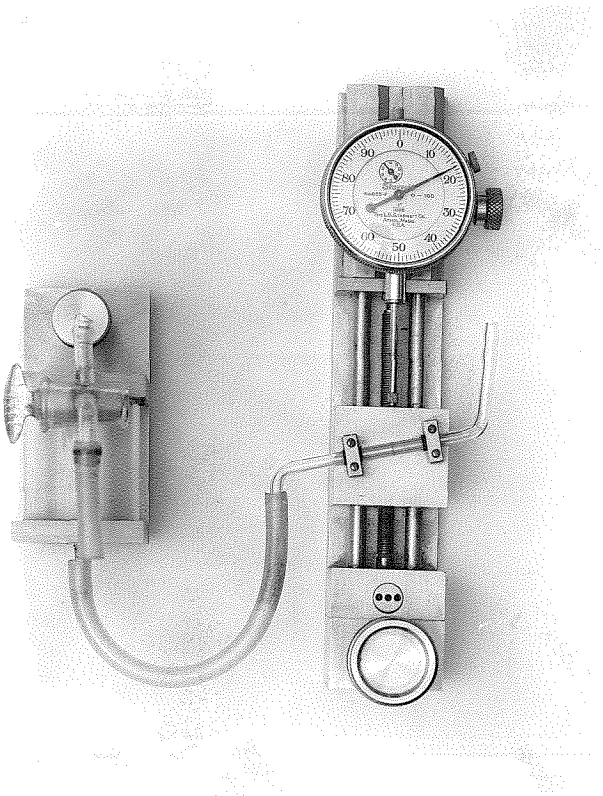

Figure 4. Micromanometer

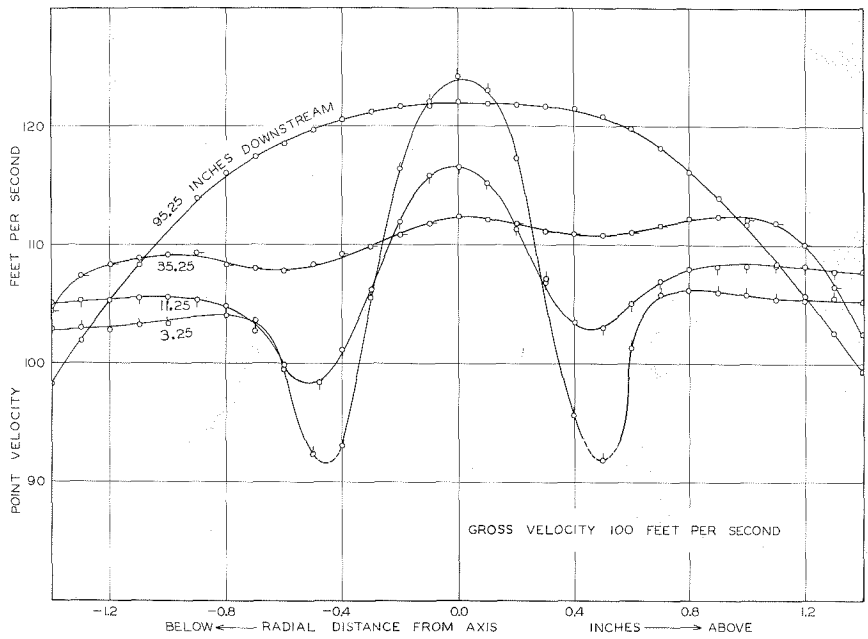

Figure 5. The Variation of Velocity with Radial Distance from the Axis of the Working Section

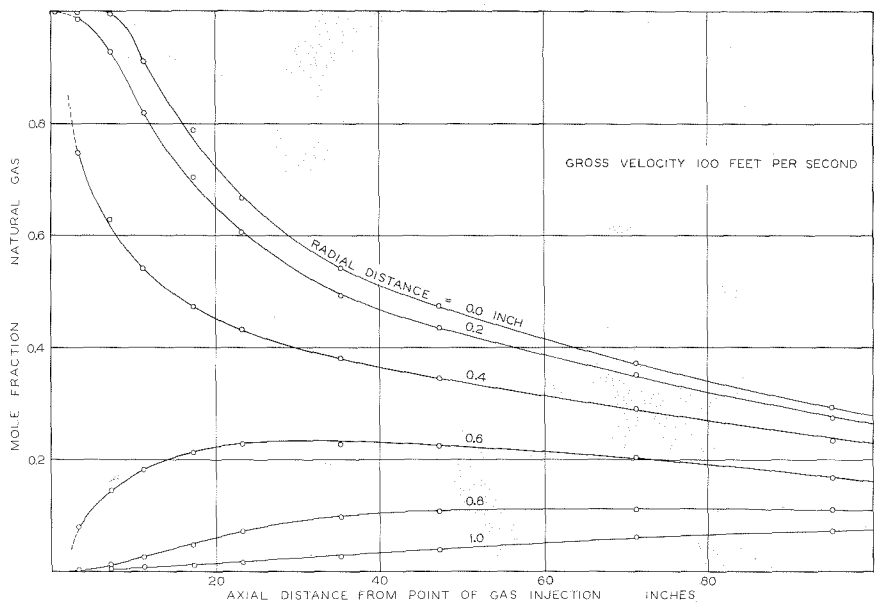

Figure 6. The Variation of Composition with Axial Distance from the Point of Initial Mixing

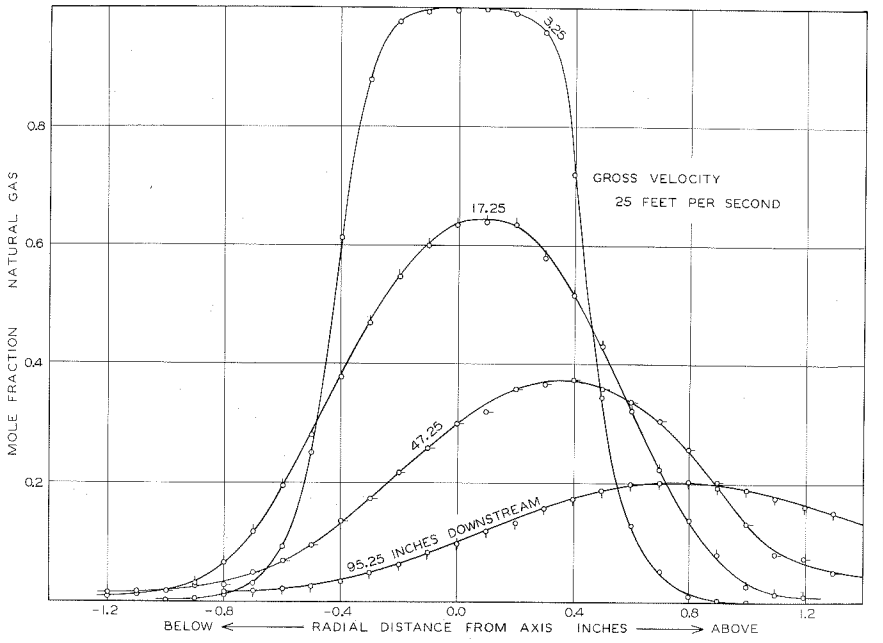

Figure 7. The Variation of Composition with Radial Distance from the Axis

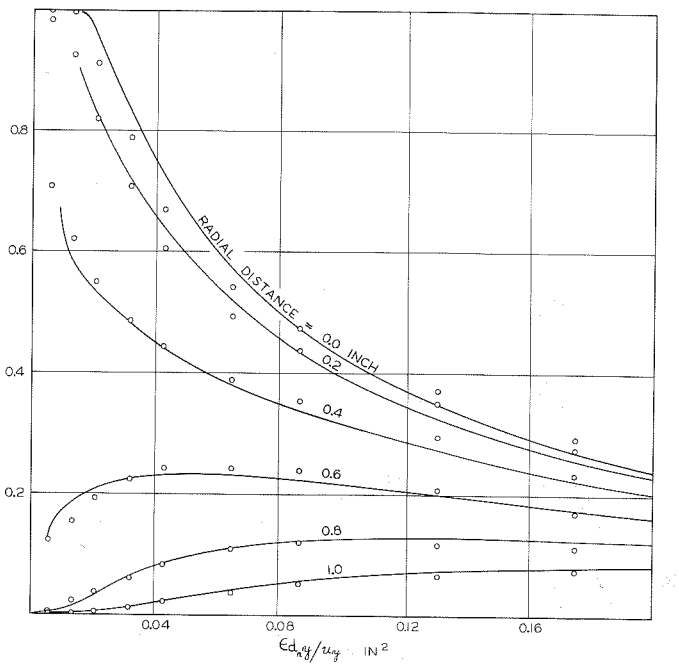

Figure 8. Comparison of Experimental Compositions (points) and Predicted Compositions (solid lines)

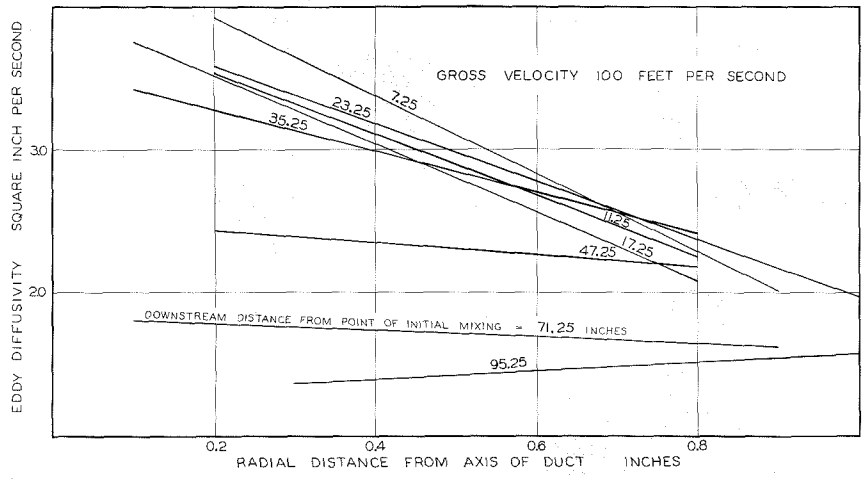

Figure 9. The Variation of Eddy Diffusivity at the Gross Velocity of 100 Feet Per Second

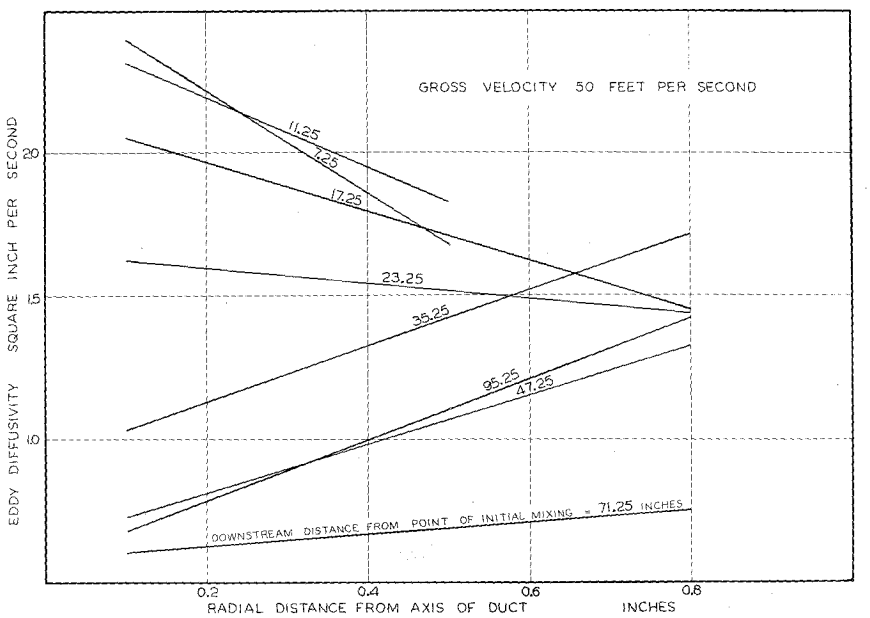

Figure 10. The Variation of Eddy Diffusivity at the Gross Velocity of 50 Feet Per Second

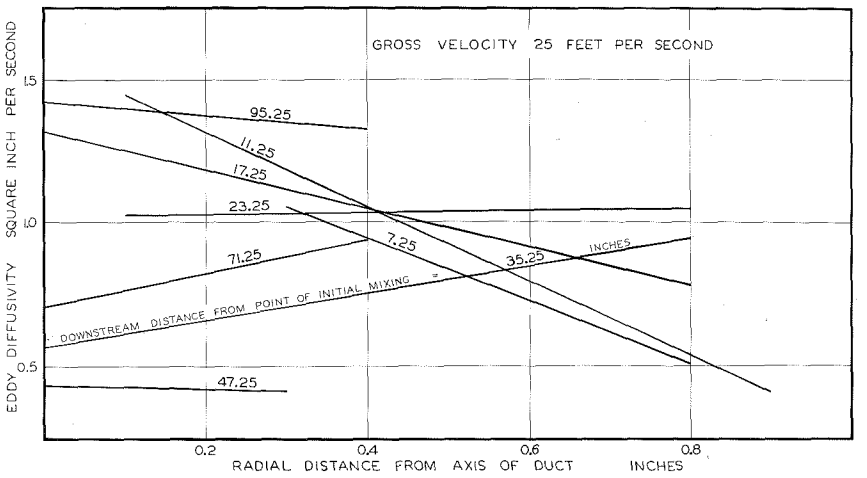

Figure 11. The Variation of Eddy Diffusivity at the Gross Velocity of 25 Feet Per Second

Propositions Submitted by Warren G. Schlinger

Ph.D. Oral Examination, May 26, 1949, 1:15 p.m., Room 156 Crellin
Committee: Professor Sage (Chairman), Professors P. Kyropoulos, Lacey, Lindvall, Pauling, Swift, Yost

1. Experimental work is now in progress in which the apparatus described in the third part of this thesis is used to study the effects produced by igniting the natural gas as it enters the working section. Measurements of composition, velocity, and temperature are being made. It is desirable to estimate the magnitude of the eddy diffusivity under the burning conditions. The following method is suggested. The two following equations*

$$div(C\vec{u}) = \frac{\partial}{\partial r}\left(r \epsilon_{dr} \frac{\partial C_2}{\partial r}\right) + \frac{\partial}{r \partial \theta}\left(\epsilon_{d\theta} \frac{\partial C_2}{\partial \theta}\right) + \frac{\partial}{\partial z}\left(r \epsilon_{dz} \frac{\partial C_2}{\partial z}\right)$$

$$div\left(\frac{\vec{u}}{T}\right) = 0$$

combined with suitable restrictions and necessary assumptions yield the relation

$$\frac{\partial^2 C_2}{\partial r^2} + \frac{1}{r}\frac{\partial C_2}{\partial r} = \frac{u_z}{\epsilon_{dr}}\frac{\partial C_2}{\partial z}$$

This equation may be solved analytically (see Part III, p 67 of this thesis) to obtain theoretical composition patterns. The experimental data may be fitted to the theoretical curves, and the average value of the eddy diffusivity estimated.

2. The "continuity equation" often expressed in the differential form (1)

$$div(\rho\vec{u}) + \frac{\partial \rho}{\partial \tau} = 0$$

and applied to compressible fluid flow cannot be applied to systems in which diffusional processes are occurring.

3. A rapid method of graphical differentiation of experimentally established curves is proposed. The technique, which requires a drafting machine, provides slopes or derivatives which are reproducible to within 1 per cent when

---

* See nomenclature in Part III of this thesis

obtained from curves with inclinations in the range of 20 to 70 degrees. The derivative is obtained by making one reading from the graphical plot and if desired conversion factors or constants may be combined with the same operation.

4. The volumetric behavior of chlorine at elevated temperatures and pressures may be accurately established by employing the apparatus described in Part I of this thesis. Such data would be of value since the industrial use of chlorine is becoming increasingly important, and data available in the literature (2) are not entirely consistent.

5. The curricula of the undergraduate applied chemists at the California Institute of Technology and also the fifth-year chemical engineering students should include more applied mathematics. It is suggested that emphasis be placed upon the solution of partial differential equations by both approximate and analytical methods.

6. The analysis made by Williams (3) on the determination of specific heats of volatile liquids is not entirely correct and may lead to errors of 1 to 2 per cent. It is believed that the heat losses during the cooling period are not equal to the heat losses during the heating period.

7. The computation of the point-to-point variation of the eddy diffusivity by fitting the experimentally established concentration distribution downstream from a point source with the error function (4) is to be avoided. It is shown (5) by theoretical considerations that the error function describes the concentration distribution when it is assumed that the eddy diffusivity is invariant in the region considered. The method serves only to obtain qualitative information concerning the variation of the diffusivity.

8. Knocking characteristics of internal combustion engine fuels are generally attributed to preflame front ignition. Knock inhibiting agents are added whose main objective is to reduce preflame front oxidation. Antiknock characteristics could also be obtained by increasing the velocity of the flame front. The following cases might be determining:

1. Increase the turbulence in the combustion chamber
2. Provide the optimum geometrical shape of the combustion chamber
3. Consider the correlation between free hydrogen atoms and flame velocity, and additives which might affect the concentration of this component

9. It is suggested that the equilibrium between nitrogen dioxide and nitrogen tetroxide at elevated pressures and temperatures be studied by comparing the measured volumetric behavior obtained under equilibrium conditions (see Part I of this thesis) with that predicted from the laws of corresponding states (6) using carbon dioxide as a comparison material.

-ooOoo-

(1) Sokolnikoff, I. S. and Sokolnikoff, E. S., "Higher Mathematics for Engineers and Physicists" McGraw-Hill Book Co., p 429 (1941).

(2) Hulme, R. E. and Tillman, A. B., Chem. Eng., 56, 99 (Jan. 1949).

(3) Williams, G. C., Ind. Eng. Chem., 40, 340 (1948).

(4) Kalinske, A. A. and Pien, C. L., Ind. Eng. Chem. 36, 220 (1944).

(5) Drew, T. B., Trans. Am. Inst. Chem. Eng., 26, 30 (1931).

(6) Gibbs, J. W., Trans. Conn. Acad., 3, 108 (1876).